Study of the plasticity of granular materials using diffusing waves spectroscopy and other works

Axelle Amon

▶ **To cite this version:**

Axelle Amon. Study of the plasticity of granular materials using diffusing waves spectroscopy and other works. Soft Condensed Matter [cond-mat.soft]. Université Rennes 1, 2014. tel-01056250

HAL Id: tel-01056250
https://theses.hal.science/tel-01056250

Submitted on 18 Aug 2014

HAL is a multi-disciplinary open access archive for the deposit and dissemination of scientific research documents, whether they are published or not. The documents may come from teaching and research institutions in France or abroad, or from public or private research centers.

L'archive ouverte pluridisciplinaire **HAL**, est destinée au dépôt et à la diffusion de documents scientifiques de niveau recherche, publiés ou non, émanant des établissements d'enseignement et de recherche français ou étrangers, des laboratoires publics ou privés.

N^0 d'ordre :

Université de Rennes 1

Habilitation à diriger des recherches

Mémoire présenté par

Axelle AMON

ÉTUDE DE LA PLASTICITÉ DES MILIEUX GRANULAIRES PAR DIFFUSION MULTIPLE DE LA LUMIÈRE ET AUTRES TRAVAUX

soutenue le 2 juin 2014 devant le jury composé de :

M. Jean-Louis Barrat	Université Joseph Fourier	(Rapporteur)
M. Jérôme Crassous	Université de Rennes 1	
M. Douglas J. Durian	University of Pennsylvania	(Rapporteur)
M. Olivier Pouliquen	IUSTI, Polytech Marseille	(Président du jury)
M. Stéphane Roux	LMT, ENS Cachan	(Rapporteur)
Mme Véronique Trappe	Université de Fribourg	

Rien n'est jamais perdu tant qu'il reste quelque chose à trouver.
Pierre Dac

Remerciements

Je tiens à remercier Jean-Louis Barrat, Doug Durian, Olivier Pouliquen, Stéphane Roux et Véronique Trappe pour avoir accepté de participer à mon jury et de juger le travail présenté dans ce mémoire. C'est un immense honneur pour moi de défendre mes travaux devant eux.

Une large part du travail présenté ici est avant tout le fruit d'une collaboration avec Jérôme Crassous avec qui c'est un énorme plaisir de travailler depuis 7 ans. Ce travail de groupe n'aurait pas été possible sans l'implication d'excellents étudiants: Marion Erpelding, Roman Bertoni et Antoine Le Bouil, et est lié à des interactions avec de nombreux collaborateurs parmi lesquels je remercie tout particulièrement Eric Clément et Sean McNamara.

Merci à Pascal Panizza et Laurent Courbin de m'avoir impliquée dans leurs trafics (de gouttes) et à Denis Michel pour sa patience et nos discussions.

La plupart des expériences décrites dans ce mémoire n'auraient jamais vu le jour sans Patrick Chasle, Jean-Charles Potier et Alain Faisant dont les compétences techniques me sont précieuses. Je remercie aussi chaleureusement l'ensemble de notre pole administratif, et tout particulièrement Valérie Ferri, les Nathalie's (Chouteau, Claudel, Gicquiaux et Mabic) ainsi que Julie Nicolle pour leur immense patience face à l'insoutenable légéreté des chercheurs face au moindre document administratif.

J'ai pu au cours de ces années avoir de nombreuses interactions fructueuses au sein de l'Institut de Physique de Rennes et tout particulièrement du département Matière Molle, et je tiens à exprimer ici ma gratitude à l'ensemble de ces personnes. Tout particulièrement, mes remerciements vont à Arnaud Saint-Jalmes pour son excellent travail de coordination à la tête du département, aux "jeunes" pour leur énergie, leur bonne humeur et leur excellente compagnie, à Isabelle Cantat avec qui c'est toujours un plaisir de parler sciences pour "éclaircir" ses idées suivant le concept de "l'effet concierge" et, *last but not least*, à Benjamin Dollet avec qui j'ai eu le plaisir jusqu'à fort récemment de partager un bureau et que je remercie d'une part pour les discussions scientifiques enrichissantes mais aussi pour supporter stoïquement mes innombrables râleries de maître de conférences surchargé.

Et pour tout "le reste", merci aux amis et surtout à François.

Contents

General introduction **9**

I Scientific career **11**

1 Short overview & CV **13**

2 Publications **19**

II Research works & projects **25**

1 Multiple scattering of light **27**
1.1 State of the art . . . 27
1.1.1 Diffusing-Wave Spectroscopy . . . 28
1.1.2 Transport mean free path . . . 30
1.2 Measurements of minute deformation . . . 31
1.2.1 Modeling of the autocorrelation function . . . 31
1.2.2 Spatial resolution . . . 34
1.2.3 Validation of the method . . . 35
1.3 Other studies concerning scattering . . . 37
1.3.1 Wavelength as a tunable parameter . . . 37
1.3.2 Scattering and chirality . . . 39

2 Plasticity in granular materials **41**
2.1 State of the art . . . 41
2.1.1 Disordered materials . . . 41
2.1.2 Elasticity and plasticity of amorphous materials . . . 43
2.1.3 Granular materials: common points and specificities . . . 47
2.2 Mechanical response of granular materials . . . 50
2.2.1 Plastic flow in a granular sample at small deformation . . . 51
2.2.2 Micro-ruptures . . . 58
2.2.3 Towards elasticity . . . 62
2.3 Work-in-progress and projects . . . 66
2.3.1 Elastic limit, cycles and contact plasticity . . . 66
2.3.2 Coupling of local rearrangements and shear-band formation . . . 67

2.3.3 "Mechanical noise" and fluidity 67

3 Nonlinear dynamics **69**
3.1 Traffic and microfluidics 70
3.2 Gene regulation 72

General conclusion **75**

Bibliography **86**

General introduction

In this dissertation I expose my main works of research since my obtention of a position as an Assistant Professor at the Institut de Physique de Rennes in 2004. My research activities during this period can be divided in three main themes: propagation of waves in heterogeneous materials, mechanical properties of granular media and nonlinear dynamics. I will focused more particularly in this dissertation on the two first sujects which correspond to my more recent works and which underlie my research projects for the next few years.

Actually, since the beginning of my PhD in 2000, I have worked in fields as diverse as nonlinear optics, light scattering, granular materials or microfluidic. This diversity is the result of a combination of curiosity, pleasure to work with different people and above all an interest for subjects not connected to a very high degree of specialization but rather implying experiments "at the human scale" where theoretical and numerical modeling can be done simultaneously with the experiment. It is exactly the suitable turn of mind to explore the field of the mechanics of granular materials. Indeed, even if large advances have been done since the renewed interest that the physicist community as shown for this field in the 90's, large parts of the mechanical properties of granular materials are still to be understood.

The document is divided in two main parts. The first one (Part I, *Scientific career*) gathered factual data concerning my scientific career: a brief historical overview, my Curriculum Vitæ and my list of publications. The second and main part of this dissertation (Part II, *Research works & Projects*) is the presentation in three chapters of my main axes of research. Chapter 1 concerns wave propagation in heterogeneous materials and scattering. Chapter 2 is about the plasticity of granular materials. Both of those chapters begin with a short state of the art. Each of their central parts are a presentation of my works in those fields. The second chapter, about granular materials, is concluded by a section concerning my future projects, which are in the continuity of my present works in the field. The last chapter (Chap. 3) is a brief overview of my recent activities linked to nonlinear dynamics.

Part I

Scientific career

Chapter 1

Short overview & CV

My research career can be roughly decomposed in two parts. From 2000 to 2007 I have worked in the field of nonlinear optics, first during my PhD in the laboratory PhLAM (Physique des Lasers, Atomes et Molécules, UMR 8523, Université de Lille 1) from 2000 to 2003, then, from 2004 to 2007, as an Assistant Professor at IPR[1] (Institut de Physique de Rennes, UMR 6251, Université de Rennes 1). My principal research interest was the study of the temporal dynamics of several nonlinear optical systems: optical parametric oscillators and lasers, with a particular interest for temporal instabilities and chaos. Between the end of my PhD thesis and my recruitement in a permanent position, I spent one year at IRPHE (Institut de Recherche sur les Phénomènes Hors Equilibre, UMR 6594, Marseille) where I have studied instabilities in flame fronts and familiarized with spatio-temporal instabilities.

At the beginning of the year 2007, I began a collaboration with Jérôme Crassous who had then recently obtained a Professor position at IPR. In the following years, we developped a method of measurement of small deformation in scattering material which principle is detailed in chapter 1. This method has allowed us to study the mechanical response of granular materials, which has became my principal research interest during the past few years. Those studies are exposed in chapter 2. In parallel, I have worked on the theoretical and numerical modeling of different nonlinear systems in collaboration with experimentalists. Those works, concerning respectively traffic in micro-fluidic networks and gene regulation are summerized in chapter 3.

During all those fourteen years, I had a continuous teaching activity. The detailed discussion of this part of my work is out of the scope of this dissertation but it does not mean that it is an insignificant part of my job. My involvement as a teacher led me to set up new lab works experiments, to write detailed lectures notes for my master students, to supervise internships of undergraduate students but also to participate to science popularization campaigns and pedagogical activities.

The highlights of my career are summerized in the following four-pages Curriculum Vitæ.

[1] In fact, first in the laboratory PALMS (Physique des Atomes, Lasers, Molécules et Surfaces, UMR 9927) which has merged in 2008 with the GMCM (Groupe matière condensée et matériaux, UMR 6626) to form the Institut de Physique de Rennes.

Curriculum Vitae

AMON Axelle – Assistant Professor
Institut de Physique de Rennes – UMR 6251
Université de Rennes 1
Bât. 11A – Campus de Beaulieu
F-35042 Rennes

born 09/29/1976 in Poissy (France, 78)
Email : axelle.amon@univ-rennes1.fr
Tel : +33 (0)2 23 23 50 38

Education & Career

since 2004 Assistant Professor, Institut de Physique de Rennes (IPR UMR 6251), Université de Rennes I.

2003–04 Lecturer (1/2 ATER) at the Institut Universitaire de Technologie of Aix-Marseille III. Research at the Institut de Recherche sur les Phénomènes Hors Equilibre (IRPHE UMR 6594).

2000–03 PhD Thesis (AMX) at the Laboratoire de Physique des Lasers, Atomes et Molécules (PhLAM UMR 8523), Université de Lille I. Supervisors : M. Lefranc et J. Zemmouri. Grade : *Mention très honorable, avec les félicitations de jury.* Distinction : Prix de thèse 2003 de Sciences Physiques de l'Ecole Doctorale Sciences de la Matière, du Rayonnement et de l'Environnement.

1999–00 DEA (Master) Champs, Particules, Matières, Université Paris 11, (Orsay, France).

1996–99 Ecole Polytechnique (Palaiseau, France).

Research Interests

- Granular matter (publications n°1,3,6,10,11)
- Plasticity, localization of deformation (n°1,3,6,10)
- Wave propagation in heterogeneous medias (n°4,7,10,11,13)
- Nonlinear dynamics : optics (n°12,14-17) traffic in microfluidics (n°2,9), gene regulation (n°5,8)

Skills

- Experiments : granular materials, optics
- Numerics : data and image analysis, ODE
- Theory : modeling, nonlinear dynamics

Organization

since 2012 Member of the organizing committee of the Summer School *"Nonlinear Dynamics in Peyresq"* (`http://www.enlpeyresq.u-psud.fr/`).

since 2010 Organizer of high level ∼3-days lectures for IPR :
2014 A. Boudaoud, ENS Lyon, *"Morphogenesis"*.
2013 J. H. Snoeijer, University of Twente, *"Capillary flows"*.
2011 F. Lequeux, ESPCI-ParisTech, *"Rheology"*.
2010 T. Erneux, Université Libre de Bruxelles, *"Dynamical systems with delay"*.

dec. 2013 Co-organizer of a one-day internal workshop for the Soft Matter Group .

2010–13 Organizer of the workgroup of the Soft Matter Group.

Collaborations

International

since 2012 Member of the *Compgram* network coordinated by M. Sperl (Institute of Materials Physics in Space, German Aerospace Center) concerning the development of a DWS measurement setup on the "FOAM-C" module on ISS.

march 2011 Visitor for a month in F. Scheffold's *Soft Matter and Photonics* group in University of Fribourg (Switzerland).

2001 Visitor during a month in the group *Optique Nonlinéaire Théorique* of the Université Libre de Bruxelles (Belgium), collaboration with T. Erneux.

National

GDR Participation to the workgroups (GDR) *Méphy* (Mechanics and Physics of Complex Systems) and *Transnat* (Natural Solid Transport).

since 2012 J. Weiss (LGGE UMR 5183, UJF, Grenoble) et D. Amitrano (ISTerre UMR 5275, UJF, Grenoble). Fractures, localization of deformation. *1 article submitted.*

since 2010 E. Clément (PMMH UMR 7636, ESPCI). Creep and shear-bands in granular materials. *1 published article.*

since 2010 C. Viggiani et P. Bésuelle (L-3SR UMR 5521, UJF, Grenoble). Biaxial tests on granular materials. *1 published article.*

Université de Rennes 1

depuis 2010 D. Michel (*Interactions Cellulaires et Moléculaires*, UMR 6026). Genes regulation. *2 published articles.*

Institut de Physique de Rennes

since 2013 J. Fade *(Optics and Photonics Group)*. Multiple scattering in the infrared domain.

since 2012 S. McNamara *(Discrete Media Group)*. Localization of the deformation. *1 article submitted.*

since 2009 P. Panizza and L. Courbin *(Soft Matter Group)*. Traffic in microfluidics networks. *3 published articles, including 1 of science popularization.*

since 2007 J. Crassous *(Soft Matter Group)*. Granular matter, wave propagation in heterogeneous materials. *7 published articles, 1 article submitted.*

Fundings

2013–14 Obtained funds from Université Rennes 1 *(Action incitative - Projets scientifiques émergents). "Rheology of granular materials : models and experiments"*, 8 k€.

2012 Obtained funds from Université Rennes 1 *(Collaborations internationales)*, for the initiation of a collaboration with M. Sperl (Institute of Materials Physics in Space, German Aerospace Center), 2 k€.

2010–14 Involved (50% of research worktime) in the grant *"Stability loss in Granular Media"* (ANR STABINGRAM), collaboration between the laboratories FAST (UMR 7608, Orsay), LAUM (UMR 6613, Le Mans), Géosciences Rennes (UMR 6118, Rennes) and IPR (UMR 6251, Rennes), 586 k€.

2010 Obtained grant from CNRS (PEPS), *"Droplet traffic in microfluidic networks"*, 3 k€.

Administrative tasks

2013 Member of the selection board in charge of the hiring of an assistant professor for the applied mechanics laboratory (LARMAUR, now part of IPR) in Rennes (France).

2006–08 In charge of the undergraduates internships (3rd year in Physics).

Supervision (since 2007)

PhD

2011–14 A. Le Bouil (co-supervision, J. Crassous 50%, A. A. 50%), *"Detection of rupture precursors using light scattering"*.

2007–10 M. Erpelding (co-supervision, J. Crassous 50%, A. A. 50%), *"Experimental study of micro-deformation in heterogeneous materials using light scattering"*.

Master 2nd year

2010 R. Bertoni, *"Avalanche precursors detection using light scattering"*.

2008 I. Hussein, *"Shear instability in bidisperse granular flow"* (with A. Valance et R. Delannay).

Master 1st year

2012 A. Maillocheau et R. Allio, *"Optical diagnostic of the deformation of granular materials using infrared waves scattering"* (with J. Fade).

2010 J. Bonte *"Droplets traffic at a junction"* (avec P. Panizza).
I. Bergonzi *"Sedimentation of glass beads suspension, permeability measurements"* (with J. Crassous).

2009 O. Jouet *"Jules Violle's actinometer"* (with D. Bernard).

Undergraduates

since 2007 5 undergraduates internships supervision.

Science Education

2013 Publication of an article in *Reflets de la physique* (edited by the French Physical Society and the Physics section of the CNRS).

2012 Organizer of experimental demonstrations for the city of Rennes *Festival des Sciences* (organized by Rennes Métropole during the *Fête de la Science*), coordination of 17 contributors, setup of experiments aimed for a broad audience.

2009 Organizer of experimental demonstrations about granular matter for schools, *"Des grains à surveiller, lumière sur leurs petits déplacements"* for the *Festival des Sciences*, with M. Erpelding and S. Bourlès.

2007–09 Supervision of 3 internships in connection with the Ancient Instruments and Books Collections of the University (renovation and use of the instruments). Publication of an article in the *Bulletin of the Scientific Instrument Society*.

2007 Co-organizer of an exposition at the University Library about ancient optical instruments and their operation.

since 2004 Yearly participation to various campaigns for prospective students (Open Days at University, informations intend to high schools students) and for Science Education.

Teaching Activities [1]

since 2004 **Assistant Professor** (192h/yr) [2], **Université Rennes 1**

Obtained teaching sabbaticals (reduction of teaching duties to 96h/yr) :
2011–13 (half-detachment to the CNRS) ;
2007–09 (from Université Rennes I (CRCT)).

- M2 lectures "Nonlinear dynamics and chaos" (33h/yr since 2007). *Redaction of lectures notes in English.*
- Training for "Agrégation de Physique" [3], lectures and lab works (M2, 30h to 45h/yr since 2007).
- Continuum mechanics (TD, M1 and L3, 20h to 32h/yr since 2008).
- Waves (TP, L3, 24h to 72h/yr since 2004). *Setting-up of 3 new experimental lab works.*
- Physics for biologists (CM, L2, 16h/yr in 2010–11 and 2013-14).
- Physics of fluids (CM, M1, 12h in 2013–14).
- Mathematics, 1st year of school for the hearing aid practitioners [4](CM and TD 45h/yr, 2009–2011).
- Statistics, 2nd year of school for the hearing aid practitioners (CM and TD 15h/yr, 2009–2011).
- Quantum mechanics (TD, 24h to 48h/yr, 2004–2007).
- Wave Optics (TD, L3, 24h/yr, 2004–2007).
- Geometric Optics (L1, CM/TD/TP, 34h/yr, 2004–2007).
- Electrical networks (L1, CM/TD/TP, 30h/yr, 2004–2007).

2003–04 **Lecturer (1/2 ATER)** (96h/an), **IUT Aix-Marseille III, Génie Thermique et Energie**

- TP Thermodynamics and fluid mechanics, L1.

2000–03 **during PhD (AMX)** (64h eq. TD/an), **Université des Sciences et Technologies de Lille**

- Mechanics and Optics, TP and tutoring, L1.

1. The French University system of education is divided in three types of courses : lectures ("cours magistral", abbreviated as CM), lab works ("travaux pratiques", TP) and sessions where students solve problems in classes ("travaux dirigés", TD). Assistant Professors (Maîtres de conférences) as well as Professors have teaching duties of 192 hours per year. The education is divided in five years, the three first years form the Licence level, each years being designated respectively as L1, L2 and L3, the two last years are devoted to the Master degree (M1 and M2).
2. The numbers are given in "équivalent TD", *i.e.* the way they are finally accounted.
3. Very selective competitive examination for teaching positions in high schools
4. Ecole d'audioprothèse de Fougères, diplôme de l'Université de Rennes 1.

Chapter 2

Publications

2.1 Publications in peer-reviewed journals

2.1.1 Submitted

1. A. Le Bouil, A. Amon, S. McNamara, and J. Crassous, "Emergence of cooperativity in plasticity of soft glassy materials", ***submitted to Phys. Rev. Lett.***.

2. R. Lehoucq, J. Weiss, B. Dubrulle, A. Amon, A. Le Bouil, J. Crassous, D. Amitrano, F. Graner, "Analysis of image versus position, scale and direction reveals pattern texture anisotropy", ***submitted to J. Stat. Mech.***.

2.1.2 Published

1. A. Le Bouil, A. Amon, J.-C. Sangleboeuf, H. Orain, P. Bésuelle, G. Viggiani, P. Chasle, and J. Crassous, "A biaxial apparatus for the study of heterogeneous and intermittent strains in granular materials", ***Granular Matter*** **16**, 1 **(2014)**.

2. A. Amon, A. Schmit, L. Salkin, L. Courbin, and P. Panizza, "Path selection rules for droplet trains in single-lane microfluidic networks", ***Phys. Rev. E*** **88**, 013012 **(2013)**.

3. A. Amon, R. Bertoni, and J. Crassous, "Experimental Investigation of Plastic Deformations Before Granular Avalanche", ***Phys. Rev. E*** **87**, 012204 **(2013)**.

4. M. Erpelding, B. Dollet, A. Faisant, J. Crassous and A. Amon, "Diffusing-Wave Spectroscopy Contribution To Strain Analysis", ***Strain*** **49**, 167 **(2013)**.

5. S. Lecomte, L. Reverdy, C. Le Quement, F. Le Masson, A. Amon, P. Le Goff, D. Michel, E. Christians and Y. Le Dréan, "Unravelling Complex Interplay Between Heat Shock Factor 1 And 2 Splicing Isoforms", ***PLoS One*** **8**, (2) e56085 **(2013)**.

6. A. Amon, V. B. Nguyen, A. Bruand, J. Crassous and E. Clément, "Hot Spots in an Athermal System", ***Phys. Rev. Lett.*** **108**, 135502 **(2012)**.

7. J. Crassous, A. Amon and J. Crassous, "Circular differential scattering of polarized light by a chiral random medium", ***Phys. Rev. A*** **85**, 023806 **(2012)**.

8. F. Nicol-Benoit, A. Amon, C. Vaillant, P. le Goff, Y. le Dréan, F. Pakdel, G. Flouriot, Y. Valotaire, and D. Michel, "A Dynamic Model of Transcriptional Imprinting Derived from Vitellogenesis Memory Effect", ***Biophys. J.*** **101**, 1557 **(2011)**.

9. D. A. Sessoms, A. Amon, L. Courbin, and P. Panizza, "Complex dynamics of droplet traffic in a bifurcating microfluidic network: Periodicity, multistability, and selection rules", ***Phys. Rev. Lett.*** **105**, 154501 **(2010)**.

10. M. Erpelding, A. Amon, and J. Crassous, "Mechanical response of granular media: New insights from Diffusing-Wave Spectroscopy", ***Europhys. Lett.*** **91**, 18002 **(2010)**.

11. J. Crassous, M. Erpelding, and A. Amon, "Diffusive Waves in a Dilating Scattering Medium", ***Phys. Rev. Lett.*** **103**, 013903 **(2009)**.

12. A. Amon, P. Suret, S. Bielawski, D. Derozier, and M. Lefranc, "Cooperative Oscillation of Nondegenerate Transverse Modes in an Optical System: Multimode Operation in Parametric Oscillators", ***Phys. Rev. Lett.*** **102**, 183901 **(2009)**.

13. M. Erpelding, A. Amon, and J. Crassous, "Diffusive wave spectroscopy applied to the spatially resolved deformation of a solid", ***Phys. Rev. E*** **78**, 046104 **(2008)**.

14. A. Amon and M. Lefranc, "Mode hopping strongly affects observability of dynamical instability in optical parametric oscillators", ***Eur. Phys. J. D.*** **44**, 547–556 **(2007)**.

15. M. Brunel, A. Amon, and M. Vallet, "Dual-polarization microchip laser at 1.53 μm", ***Opt. Lett.*** **30**, 2418 **(2005)**.

16. A. Amon and M. Lefranc, "Topological signature of deterministic chaos in short nonstationary signals from an optical parametric oscillator", ***Phys. Rev. Lett.*** **92**, 094101 **(2004)**.

17. A. Amon, M. Nizette, M. Lefranc and T. Erneux, "Bursting oscillations in optical parametric oscillators", ***Phys. Rev. A*** **68**, 023801 **(2003)**.

2.2 Conference proceedings

2.2.1 International conferences

1. A. Le Bouil, A. Amon, and J. Crassous, "Experimental studies of precursors to failure in granular material", **Proceedings of Powders and Grains**, **AIP Conference Proceedings**, **1542**, 475 **(2013)**.

2. M. Erpelding, A. Amon, and J. Crassous, "Light-scattering measurements of micro-deformations in granular materials", **Proceedings of the 14^{th} International Conference on Experimental Mechanics**, **EPJ Web of Conferences 6**, 33001 **(2010)**.

3. A. Amon, R. Delannay and A. Valance, "Shear Instabilities in Bidisperse Granular Flows", Proceedings of Powders and Grains, **AIP Conference Proceedings**, **1145**, 583 **(2009)**.

4. M. Erpelding, A. Amon, and J. Crassous, "Interferometric measurements of small deformations of granular materials", **Proceedings of Powders and Grains**, **AIP Conference Proceedings**, **1145**, 237 **(2009)**.

5. A. Amon and M. Lefranc, "Topological signature of deterministic chaos in short nonstationary signals from an optical parametric oscillator", **Proceedings of the 8^{th} Experimental Chaos Conference**, **AIP Conference Proceedings 742**, 357 **(2004)**.

2.2.2 National conferences

1. A. Amon, V. B. Nguyen, A. Bruand, J. Crassous and E. Clément, "Fluage et rupture dans un matériau granulaire", **Comptes-Rendus de la 15ème Rencontre du Non-linéaire**, p. 19 **(2012)**.

2. D. Sessoms, A. Amon, L. Courbin, and P. Panizza, "Trafic de gouttes à une jonction", **Comptes-Rendus de la 13ème Rencontre du Non-linéaire**, p. 175 **(2010)**.

3. A. Amon et M. Lefranc,"Les sauts de mode tronquent la dynamique des oscillateurs paramétriques optiques", **Comptes-Rendus de la 9ème Rencontre du Non-linéaire**, p. 13 **(2006)**.

4. A. Amon, P. Suret, S. Bielawski, D. Derozier, J. Zemmouri, M. Lefranc, M. Nizette, and T. Erneux, "Instabilities and chaos in optical parametric oscillators", **Proceedings du 8^{me} colloque sur les lasers et l'optique quantique**, **Journal de Physique IV**, **119**, 113 **(2004)**.

5. A. Amon, M. Nizette, M. Lefranc et T. Erneux, "Observation expérimentale et modélisation de bursting dans les oscillateurs paramétriques optiques", **Comptes-Rendus de la 6ème Rencontre du Non-linéaire**, p. 19 **(2003)**.

6. A. Amon et M. Lefranc, "Signature topologique de chaos déterministe dans un oscillateur paramétrique optique", **Comptes-Rendus de la 6ème Rencontre du Non-linéaire**, p. 167 **(2003)**.

2.3 Science popularization and history of science

1. P. Panizza, A. Amon, and L. Courbin, "Comment circulent des gouttes dans un laboratoire sur puce ?", ***Reflets de la Physique*** **36**, 4–6 **(2013)**.

2. O. Jouet, A. Amon and D. Bernard, "Jules Violle's Actinometer : A simple instrument to deduce the temperature at the surface of the sun", ***Bulletin of the Scientific Instrument Society*** **112**, 28–30 **(2012)**.

2.4 Dissertation

1. "Dynamique temporelle des oscillateurs paramétriques optiques continus : oscillations multimodes, oscillations en rafales et chaos", A. Amon, thèse de doctorat, Université de Lille 1 (2003).

2.5 Communications

Are listed only the communications I gave myself, excluding those which I co-authored without ensuring the presentation.

2.5.1 Invitations

2.5.1.a National workshop

1. *"Diffusion multiple de la lumière dans les milieux granulaires"* for the workshop "Nouvelles technologies de caractérisation des matériaux appliquées dans le domaine cosmétique" organized by LVMH R&D (Recherche Parfums et cosmétiques), Saint-Jean-de-Braye, France **(2014)**.

2.5.1.b Seminars

1. *"Local rearrangements and failure in granular materials"*, Max Planck Institute for Dynamics and Self-Organization, Göttingen, Germany, **(2012)**.
2. *"Micro-déformations et formation de bandes de cisaillement dans un matériau granulaire"*, Institut des Sciences de la Terre, Grenoble, France **(2012)**.
3. *"Light-scattering measurements of micro-deformations in granular materials"*, Departement of Physics, University of Fribourg, Switzerland **(2011)**.
4. *"Trafic de gouttes à une jonction"*, Laboratoire PMMH, ESPCI, Paris, France **(2010)**.
5. *"Instabilités et chaos dans les oscillateurs paramétriques optiques"*, Laboratoire PALMS, Rennes, France **(2004)**.
6. *"Instabilités et chaos dans les oscillateurs paramétriques optiques"*, IUSTI, Marseille, France **(2003)**.

2.5.2 Talks

2.5.2.a International conferences

1. A. Amon, V. B. Nguyen, A. Bruand, J. Crassous and E. Clément, "Creep, fluidity and rupture in a granular material", WORKSHOP "MATERIAL'S DEFORMATION: FLUCTUATION, SCALING, PREDICTABILITY", Les Houches, France **(2012)**.
2. M. Erpelding, A. Amon, and J. Crassous, "Light-scattering measurements of micro-deformations in granular materials", 14TH INTERNATIONAL CONFERENCE ON EXPERIMENTAL MECHANICS (ICEM14), Poitiers, France **(2010)**.
3. D. Sessoms, A. Amon, L. Courbin, P. Panizza, "Droplet traffic at a junction: dynamics of path selection", 11TH EXPERIMENTAL CHAOS AND COMPLEXITY CONFERENCE (ECC11), Lille, France **(2010)**.
4. A. Amon, M. Lefranc, M. Nizette, T. Erneux, "Bursting in optical parametric oscillators", EUROPEAN QUANTUM ELECTRONICS CONFERENCE (EQEC) 2003, Münich, Allemagne **(2003)**.

2.5.2.b National conferences

1. A. Le Bouil, A. Amon, S. McNamara, and J. Crassous, "Microstructure of plastic granular Flow", workshop GDR Méphy "Jamming, 15 ans plus tard", Paris, France **(2013)**.
2. A. Amon, R. Bertoni, and J. Crassous, "Précurseurs à la déstabilisation d'un empilement granulaire", réunion générale du GDR Méphy, Agay, France **(2012)**.
3. D. Sessoms, A. Amon, L. Courbin, P. Panizza, "Trafic de gouttes à une jonction", 13ème Rencontre du non linéaire, Paris **(2010)**.
4. A. Amon, M. Nizette, M. Lefranc et T. Erneux, "Observation expérimentale et modélisation de bursting dans les oscillateurs paramétriques optiques", 6ème Rencontre du non linéaire, Paris **(2003)**.

2.5.3 Posters

2.5.3.a International conferences

1. A. Amon, R. Bertoni, and J. Crassous, "Destabilization of a granular pile", workshop "Material's deformation: Fluctuation, Scaling, Predictability" 2nd edition, Les Houches, France **(2013)**.
2. A. Amon, V. B. Nguyen, J. Crassous and E. Clément, "Creep, fluidity and rupture in a granular material", GRC Granular & Granular-Fluid Flow 2012, Davidson College, North Carolina, USA **(2012)**.
3. A. Amon, D. Sessoms, L. Courbin, and P. Panizza, "Traffic of droplets in microfluidic networks", GRC Soft Condensed Matter Physics 2011, Colby-Sawyer College, New Hampshire, Etats-Unis **(2011)**.
4. A. Amon, R. Delannay, and A. Valance, "Shear instabilities in bidisperse granular flows", Powders and Grains 2009, Denver, Colorado, USA **(2009)**.
5. M. Erpelding, A. Amon, and J. Crassous, "Interferometric measurements of small deformations of granular materials", Powders and Grains 2009, Denver, Colorado, USA **(2009)**.
6. R. M. Guillermic, R. Delannay, A. Valance and A. Amon, "Shear instabilities in bidisperse granular flows", GRC Granular & Granular-Fluid Flow 2008, Colby College, Maine, USA **(2008)**.
7. A. Amon, G. Searby and J. Quinard, "Response of premixed flames to high frequency acoustic waves", 30^{th} International Symposium on Combustion, Chicago, Illinois, USA **(2004)**.

2.5.3.b National conferences

1. A. Le Bouil, J. Crassous, S. McNamara, and A. Amon, "Structuration de la plasticité dans un milieu amorphe", 17ème Rencontre du Non-linéaire, Paris **(2014)**.
2. A. Amon, V. B. Nguyen, J. Crassous and E. Clément, "Fluage et rupture dans un matériau granulaire", 15ème Rencontre du Non-linéaire, Paris **(2012)**.

3. A. Amon, R. Delannay et A. Valance, "Instabilités d'écoulements granulaires bidisperses en cisaillement sur un plan incliné", 12ème Rencontre du non linéaire, Paris **(2009)**.

4. A. Amon, P. Suret, S. Bielawski, D. Derozier and M. Lefranc, "Caractère multimode d'un oscillateur paramétrique optique triplement résonant", 10ème Rencontre du non linéaire, Paris **(2007)**.

5. A. Amon et M. Lefranc, "Les sauts de mode tronquent la dynamique des oscillateurs paramétriques optiques", 9ème Rencontre du non linéaire, Paris **(2006)**.

6. M. Brunel, A. Amon et M. Vallet, "Quelques bénéfices tirés des effets thermiques dans les lasers à solide", 9ème colloque sur les lasers et l'optique quantique, Dijon, France **(2005)**.

7. A. Amon et M. Lefranc, "Signature topologique de chaos déterministe dans un oscillateur paramétrique optique", 6ème Rencontre du non linéaire, Paris **(2003)**.

8. A. Amon, S. Bielawski, D. Derozier, T. Erneux, M. Lefranc, M. Nizette, P. Suret, J. Zemmouri, "Retard à la bifurcation dans les oscillateurs paramétriques optiques", 7ème Colloque sur les Lasers et l'Optique Quantique, Rennes **(2001)**.

9. A. Amon, S. Bielawski, D. Derozier, T. Erneux, M. Lefranc, M. Nizette et J. Zemmouri, "Retard à la bifurcation dans les oscillateurs paramétriques Optiques", 4ème Rencontre du non linéaire, Paris **(2001)**.

Part II

Research works & projects

Chapter 1

Multiple scattering of light

Jérôme Crassous and myself have developed the past few years at the Institut de Physique de Rennes a method of measurement of heterogeneous deformations in scattering materials. This work has been first initiated by J. Crassous in Lyon [Djaoui and Crassous, 2005] and its development and implementation has marked the beginning of our collaboration in Rennes from 2007 and has been the subject of the PhD thesis of Marion Erpelding [Erpelding, 2010] that we co-supervized from 2007 to 2010.

The method is based on *Diffusing-Wave Spectroscopy* (DWS) [Pine, 2000] and aims at the visualization of heterogeneous minute deformation in athermal scattering materials, *i.e.* when the brownian motion of the scatterers is negligible. Spatial resolution is obtained in near field by taking advantage of the peaked statistical distribution of the light paths lengths around a typical length in the backscattering configuration.

In this chapter, I will first present the general principles of DWS. In a second part I detail our method and give some examples of the tests we have performed to validate the measurements. Finally, I give a brief overview of some of our other works linked to waves propagation in heterogeneous materials.

1.1 State of the art

The study of the rheology of soft matter (dense colloidal suspensions, emulsions, foams, granular materials) have benefited from recent advances in diverse optical technics [Cipelletti and Weeks, 2011]. As all those materials strongly scatter light because of their heterogeneous nature, light scattering techniques have became favored non-intrusive methods of measurement of their structure and dynamics [Pine, 2000]. The development of those methods, first in the case of single scattering in dilute suspension leading to the development of Dynamical Light Scattering (DLS) and then its extension to the case of multiple scattering with Diffusing-Wave Spectroscopy (DWS) [Weitz and Pine, 1993; Maret, 1997] have led to large advances in the understanding of the dynamics first of dense colloidal suspensions [Maret and Wolf, 1987; Pine et al., 1988, 1990], and then of other materials [Durian et al., 1991; Menon and Durian, 1997; Hébraud et al., 1997].

1.1.1 Diffusing-Wave Spectroscopy

Numerous disordered media, as foams, grains or concentrate colloidals suspensions, because of their heterogeneities, strongly scatter light. Light rays follow different paths in the material, each path being composed of numerous scattering events (see Fig. 1.1). When the source is coherent, the transmitted and backscattered light give rise to interferences and the collected intensities display fluctuations corresponding to interferences originating from a disordered system: a speckle figure (see Fig. 1.1). Those scattered light rays have performed a random walk inside the material and thus have explored a part of the bulk of the material. The method discussed here consequently differ from technics based on speckles arising from mere surfacic irregularities which provides only surfacic information [Dainty, 1984].

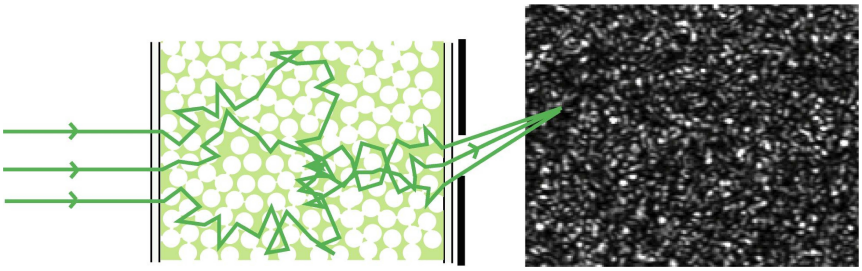

Figure 1.1: Left: an example of a scattering material, here glass beads. Light rays inside the material follow complicated paths made of numerous reflection and refraction events. Right: the collected rays interfer resulting in a speckle image.

If the system has an internal dynamics (typically brownian motion for a colloidal suspension) the speckle figure will change with time. The principle of the *Diffusing-Wave Spectroscopy* (DWS) is to analyse the fluctuations of the scattered intensity to extract information about the structure or dynamics of the system [Pine, 2000; Weitz and Pine, 1993].

The principle of the analysis is based on the calculation of the auto-correlation function g_I of the scattered intensities. The correlations are calculated between two states of the sample we will call 1 and 2 in the following[1]:

$$g_I(1,2) = \frac{\langle I_1 I_2 \rangle}{\langle I_1 \rangle \langle I_2 \rangle} \tag{1.1}$$

The average operation $\langle \cdot \rangle$ in Equation 1.1 can be performed over time (it is then supposed that the phenomenon studied is ergodic), or over an ensemble of speckles [Scheffold and Cerbino, 2007]. In the multi-speckles method [Viasnoff et al., 2002], light intensity is collected on a CCD camera, each speckle being an independent representation of the same random process and an ensemble average is obtained by averaging over the pixels of the camera.

Because of the inner dynamics, a loss of correlation between two speckle figures corresponding respectively to two different states of the material is measured (see Fig. 1.2). As strong scattering is at play, no information on the details of the scattering process inside the material can be infered, contrary to single scattering technics. Nevertheless, informations can still be extracted through a

[1] To avoid confusion with the designation of the states (1 and 2), I will use the notations g_E and g_I to designate the correlations calculated respectively on the amplitudes E and intensities I of light instead of the usual notations g_1 and g_2.

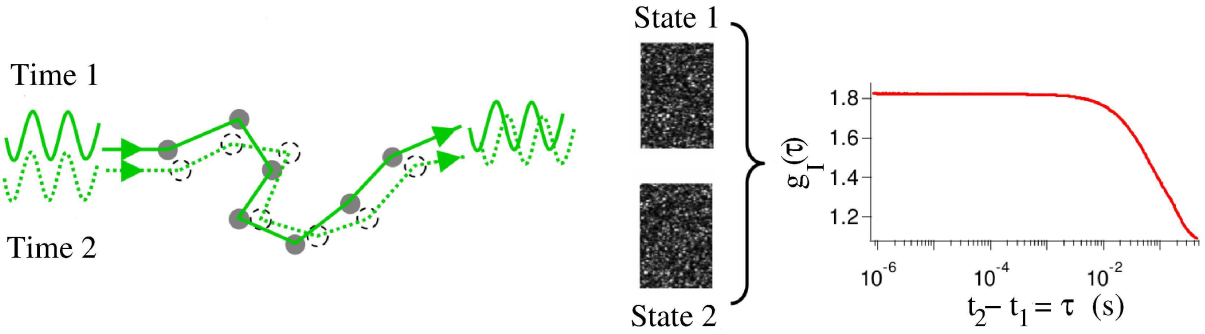

Figure 1.2: From [Erpelding, 2010]: principle of Diffusing Wave Spectroscopy. Because of some inner dynamics, a relative modification of the positions of the scatterers occur during time. Each configuration of the structure of the material gives a different speckle image. The calculated correlation function of the transmitted intensity $g_I(\tau)$ between the intensities $I_1 = I(t)$ and $I_2 = I(t+\tau)$ decreases with the time lag τ. The curve has been obtained during the ageing of a shaving foam.

modeling of the propagation of light in the material. In the case of strong scattering, the models describing the light propagation in the sample are based on the hypothesis that the propagation of the light inside the sample can be described as a diffusion process [Ishimaru, 1978]. Although the diffusion process causes the loss of most of the detailed information about the material in which it propagates, this process is also at the origin of the unmatchable sensitivity of the method. Usually, the sensitivity of an interferometric method is of the order of the wavelength of the coherent source used. Indeed, a loss of correlation between two interferometric figures corresponds typically to the change from constructive interferences to destructive ones, *i.e.* to a change between the ray paths of the order of the wavelength. But as multiple scattering implies a large number of scattering events, decorrelation will occur when the scatterers will have move only of a fraction of the wavelength. Consequently, relative displacements of a few nanometers of the scatterers are measurable [Weitz and Pine, 1993].

The calculation of the theoretical g_I and g_E can be rather complicated. The outline of such a calculation in the case of interest for our method will be given in the next section. In this general section, I will just expose here an important feature of the correlation calculation common to DLS and DWS. Consider the field at a point on a sensor, its amplitude E is the sum of a large number of rays $E(t) = \sum_\alpha \mathcal{E}_\alpha(t)$. The cross term of the amplitude correlation is:

$$\begin{aligned} E(t_1)E^*(t_2) &= \left(\sum_\alpha \mathcal{E}_\alpha(t_1)\right)\left(\sum_\beta \mathcal{E}^*_\beta(t_2)\right) \\ &= \sum_\alpha \mathcal{E}_\alpha(t_1)\mathcal{E}^*_\alpha(t_2) + \sum_{\alpha\neq\beta} \mathcal{E}_\alpha(t_1)\mathcal{E}^*_\beta(t_2) \end{aligned}$$

When averaging, the contribution from $\sum_{\alpha\neq\beta}\left\langle \mathcal{E}_\alpha(t_1)\mathcal{E}^*_\beta(t_2)\right\rangle$ will vanish because the fields $\mathcal{E}$

originating from different paths ($\alpha \neq \beta$) can be considered as uncorrelated. Consequently:

$$\begin{aligned} \langle E(t_1)E^*(t_2)\rangle &= \sum_\alpha \langle \mathcal{E}_\alpha(t_1)\mathcal{E}^*_\alpha(t_2)\rangle \\ &= \sum_\alpha \left\langle \mathcal{A}e^{-j\phi_\alpha(t_1)}\mathcal{A}e^{j\phi_\alpha(t_2)}\right\rangle \\ &\propto \sum_\alpha \left\langle e^{j\Delta\phi}\right\rangle \end{aligned} \tag{1.2}$$

which means that the statistical properties of the fluctuations depend only of the phase variation of each paths. Consequently, understanding the form of the correlation function necessitate to calculate the typical phase variations.

1.1.2 Transport mean free path

An important quantity that characterizes the random propagation of light in a scattering material is the transport mean free path which is usually noted l^*. In an ideal random process where each scattering event has no memory, l^* is the same as the usual mean free path (see Figure 1.3(a) and (b)). Such isotropic scattering is tyical of the Rayleigh scattering, *i.e.* the scattering of light by particles much smaller than the wavelength λ. But when the scatterers have a size of the same order than λ, the scattering process is describe by the Mie theory [van de Hulst, 1981]: light is not scattered isotropically but follow preferentially the incident direction (see Figure 1.3(c)). Several scattering events are then needed for the light to forget its incident direction (see Figure 1.3(d)).

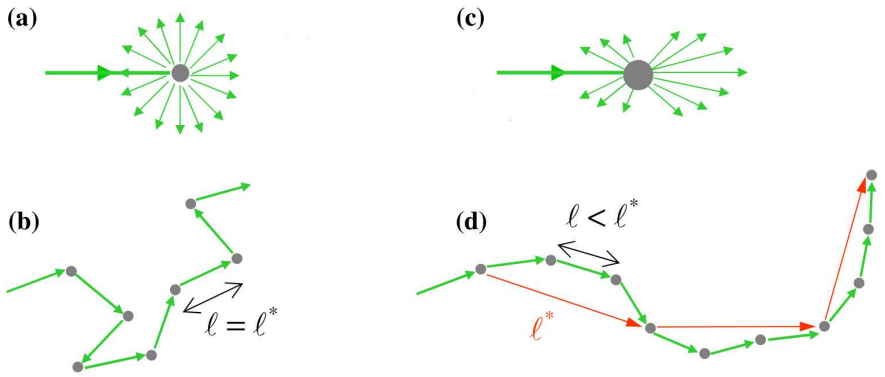

Figure 1.3: From [Erpelding, 2010]. (a) Isotropic scattering. (b) Light propagation can be modeled as a random walk of step $l = l^*$ with no correlation of orientation. (c) Mie scattering: anisotropic scattering. Because of the preferential direction of scattering, the random process has a persistent length and the total loss of memory is done on a length l^* which counted several scattering steps l.

In our works, the scattering materials are collections of glass beads of diameter d typically between 100 μm and 500 μm. The scattering process consists then in a succession of refractive or reflective events at the glass/air interfaces. The study of such scattering process has been done numerically by J. Crassous [Crassous, 2007]. He has shown that for glass beads $l^* \simeq 3.3d$.

Experimentally, measurements of the transport length l^* can be done by measuring the intensity transmitted by slabs of different thicknesses of the scattering material and comparing it to the transmission of a calibrated dispersion of latex spheres. The transmission as a function of the thickness depends then on two parameters: the absorption length and the transport mean free length l^* [Leutz and Rička, 1996]. In the following, all the values of l^* that are given for the materials we use in different experiments (Teflon, sand) have been measured using this procedure.

1.2 Measurements of minute deformation

Main associated publications:

- M. Erpelding, A. Amon, and J. Crassous, "Diffusive wave spectroscopy applied to the spatially resolved deformation of a solid", ***Phys. Rev. E*** **78**, 046104 **(2008)**.
- M. Erpelding, B. Dollet, A. Faisant, J. Crassous and A. Amon, "Diffusing-Wave Spectroscopy Contribution To Strain Analysis", ***Strain*** **49**, 167 **(2013)**.

Our method provides *spatially-resolved* measurements of small *deformations* in a scattering materials. Compared to the general framework that has been described in the previous section and which was intially based on the description of the brownian motion of colloidal suspensions, two features have to be included.

The first problematic is to take into account a deterministic displacement of the scatterers. Indeed, DWS technics have very soon included inhomogeneous flow in the scattering system [Wu et al., 1990; Bicout et al., 1991; Bicout and Maynard, 1993; Bicout and Maret, 1994]. The loss of correlation comes then both from the brownian motion of the particles and of the inhomogeneous flow field. Our modeling of the loss of correlation in our systems is based on those works. The second point is the possibility to obtain spatially-resolved measurements. We will see in the following how in backscattering and near-field configuration such a measurement is possible [Erpelding et al., 2008; Duri et al., 2009; Zakharov and Scheffold, 2010; Sessoms et al., 2010b].

1.2.1 Modeling of the autocorrelation function

1.2.1.a Principle

If experimentally the correlation is calculated over the intensities, which are indeed the quantities measured on a camera, the modeling is done by calculating the correlation function of the amplitudes:

$$g_E(1,2) = \frac{\langle E_1 E_2^* \rangle}{\langle |E_1| \rangle \langle |E_2| \rangle} \tag{1.3}$$

When the scattered field E has a gaussian distribution, the correlation functions on amplitudes and intensities are linked by the Siegert relation [Berne and Pecora, 2000]:

$$g_I(1,2) = 1 + \beta_e |g_E(1,2)|^2 \tag{1.4}$$

where β_e is an experimental constant of order unity depending on the details of the experimental setup [Berne and Pecora, 2000].

The scattered electric field E results from the superposition of contributions from different optical paths. As we have seen in the previous section (Eq. 1.2), the function $g_E(1,2)$ depends on the phase variation on each of those paths between the states 1 and 2. A variation of length Δs of a path of length s leads to a phase variation $\Delta\phi_s = k\Delta s$ for the light ray following this path, with $k = 2\pi/\lambda$ the wavevector of the light, and λ its wavelength. In the multiple scattering limit, the correlation function of the scattered field may then be expressed as [Weitz and Pine, 1993; Pine et al., 1990]

$$g_E(1,2) = \int_s \mathcal{P}(s) \left\langle e^{j\Delta\phi_s(1,2)} \right\rangle ds \tag{1.5}$$

where $\mathcal{P}(s)$ is the probability for an optical path to have the length s. This distribution can be calculated from the diffusive equation knowing the boundary conditions of the experiment [Ishimaru, 1978]. The quantity $\left\langle e^{j\Delta\phi_s(1,2)} \right\rangle$ is the contribution of a path of length s to the variation of the electric field between the states 1 and 2 and the average $\langle\cdot\rangle$ is done over all the paths of length s.

All the information about the deformation or dynamics of the material is contained in the term $\left\langle e^{j\Delta\phi_s(1,2)} \right\rangle$. The number of scattering events in each paths is large so that by the central limit theorem, $\Delta\phi_s$ is a random variable, and:

$$\langle \exp(j\Delta\phi_s) \rangle = \exp(j\langle\Delta\phi_s\rangle) \cdot \exp\left(-\frac{\langle\Delta\phi_s^2\rangle - \langle\Delta\phi_s\rangle^2}{2} \right)$$

1.2.1.b Phase variation due to affine deformation

The calculation of $\Delta\phi$ can be done by considering the displacements of the scatterers between the two states (see Fig. 1.4):

$$\Delta\phi = \phi_2 - \phi_1 = \sum_\nu \mathbf{k}_\nu^{(2)} \cdot \left[\mathbf{r}_{\nu+1}^{(2)} - \mathbf{r}_\nu^{(2)} \right] - \sum_\nu \mathbf{k}_\nu^{(1)} \cdot \left[\mathbf{r}_{\nu+1}^{(1)} - \mathbf{r}_\nu^{(1)} \right]$$

where $\mathbf{r}_\nu^{(\alpha)}$ is the position of the ν^{th} scatterers and $\mathbf{k}_\nu = k\mathbf{e}_\nu$ is the wavevector after the ν^{th} scattering event in the state number α (see Fig. 1.4).

If the scatterers move because of a displacement field $\mathbf{u}(\mathbf{r})$, we can write:

$$\Delta\phi = \sum_\nu \mathbf{k}_\nu \cdot [\mathbf{u}_{\nu+1} - \mathbf{u}_\nu]$$

where the change of direction of $\mathbf{k}_\nu$ between the two states is neglected at the first order and $\mathbf{u}_\nu = \mathbf{r}_\nu^{(2)} - \mathbf{r}_\nu^{(1)}$. When the deformation can be considered as affine, we obtain [Bicout et al., 1991; Bicout and Maynard, 1993; Bicout and Maret, 1994]:

$$\Delta\phi = k \sum_\nu l_\nu \sum_{i,j} e_{\nu,i} e_{\nu,j} U_{ij}(\mathbf{r}_\nu)$$

where $\mathbf{U}$ is the strain tensor: $U_{ij} = \frac{1}{2}\left(\frac{\partial u_i}{\partial j} + \frac{\partial u_j}{\partial i} \right)$ and $e_{\nu,i}$ are the components of the unitary vector $\mathbf{e}_\nu$.

The averages $\langle\Delta\phi_s\rangle$ and $\langle\Delta\phi_s^2\rangle$ are then calculated over the paths of same length s. For strong scattering, those averages will depend respectively on the first and the second invariants of the

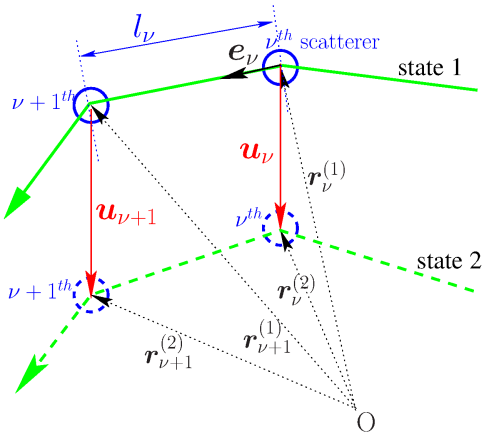

Figure 1.4: Details of the modification of the path of a light ray because of the displacement field $\mathbf{u}(\mathbf{r})$. The vectors $\mathbf{r}_\nu^{(\alpha)}$ indicate the positions of the scatterers with respect to an arbitrary origin O. The vector $\mathbf{e}_\nu$ is an unitary vector giving the direction of the wavector $\mathbf{k}_\nu$.

strain tensor $\mathbf{U}$ [Bicout et al., 1991; Bicout and Maynard, 1993; Bicout and Maret, 1994; Crassous, 2007]:

$$\langle \Delta\phi_s \rangle = \frac{1}{3} ksTr(\mathbf{U}) \tag{1.6}$$

$$\langle \Delta\phi_s^2 \rangle - \langle \Delta\phi_s \rangle^2 = k^2 s \left((\beta - \chi)\, Tr^2(\mathbf{U}) + 2\beta Tr(\mathbf{U}^2) \right) \tag{1.7}$$

where β and χ are constants of the dimension of length which depend on the details of the propagation of light in the material. They have been calculated explicitely by Bicout *et al.* in the case of Mie diffusion ($\beta = 2l^*/15$ and $\chi = 0$).

1.2.1.c Theoretical correlation function

When calculating the integral 1.5 weighted by the length distribution of the paths, the function g_E can be obtained in the backscattering configuration:

$$|g_E(1,2)| \approx \exp(-\eta k l^* \sqrt{3f(\mathbf{U})}) \tag{1.8}$$

where η is a numerical factor of order 1 taking into account polarization effects [MacKintosh et al., 1989], and:

$$f(\mathbf{U}) = \frac{\beta - \chi}{2l^*} Tr^2(\mathbf{U}) + \frac{\beta}{l^*} Tr(\mathbf{U}^2) \tag{1.9}$$

Consequently we await for the dependence of g_I:

$$g_I(1,2) \approx \exp(-c\bar{\epsilon}) \tag{1.10}$$

where the order of magnitude of the constant c can be estimated depending on the knowledge of the scattering process in the material, and $\bar{\epsilon}$ is a scalar representative of the amount of deformation in the material and linked to the quadratic invariants of the strain tensor. In the experiemnts with glass beads, we use $c = 8\pi\sqrt{3}l^*/\lambda$ to estimate a value of $\bar{\epsilon}$ from the normalized intensity correlation [Erpelding, 2010].

1.2.1.d Taking into account plasticity

The previous calculation applies in the case when the displacement of the scatterers only originate from an affine deformation. In several of our works, the question of the quantification of a plastic part has to be discussed [Crassous et al., 2009; Erpelding, 2010]. For example, in cyclic loading, it is possible to measure the unrecovered correlation when coming back in the initial state after a complete cycle, which gives the amount of irreversible processes.

Considering that the overall deformation ϵ results from the superposition of an elastic part $\mathbf{U}$ and a plastic part $\mathbf{P}$, we write [Erpelding, 2010]:

$$g_I(1,2) \approx \exp\left(-c\left(\bar{U}+\bar{P}\right)\right) \tag{1.11}$$

1.2.2 Spatial resolution

Spatial resolution can be obtained in spite of the strong scattering because in the backscattering configuration, the distribution $\mathcal{P}(s)$ is peaked around l^*: in this geometry, most of the paths only explore a small volume characterized by l^* in a sample before to leave it. As a consequence, the part of the sample that has been typically scanned by the rays emerging from the sample at a given position is a small volume $(l^*)^3$ [Baravian et al., 2005]. This property can be exploited to obtain spatial resolution in the backscattering geometry by imaging the sample on a CCD camera 1.5(a). Then, the rays interfering on the sensor are coming from the same location of the sample and carry information about a small volume of the sample. Dividing the speckle image in areas of size γl^*, we obtain subimages which we call metapixels, and which we can use individually for the multi-speckles calculation of the correlation function. We see immediately that the spatial resolution of the method is necessarily limited by l^*.

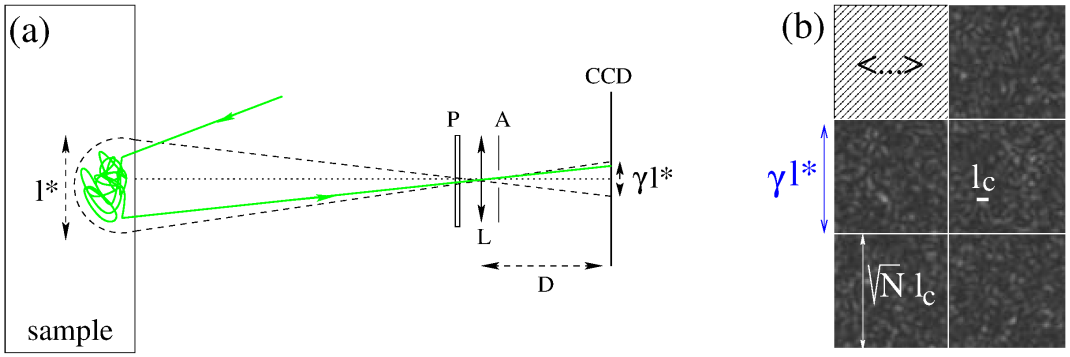

Figure 1.5: (a) Schematic of the imaging setup. Coherent light coming from an expanded laser beam (not represented) illuminates the sample. A lens L conjugates the front of the sample and the CCD sensor with a magnification γ. An aperture A allows to control independently the size of the speckles. A polarizer P can be inserted to ensure the collection of only depolarized light. (b) The speckle image obtained on the camera is divided in metapixels containing typically N speckles of typical size l_c.

Each metapixel must contain enough speckles for the multi-speckles average calculation. The control of the size of the speckles is done by inserting a diaphragm which aperture will determine the size of the speckles l_c. This size must stay large enough for the speckles to be clearly identified once pixelated [Viasnoff et al., 2002]. The resulting optical setup is represented in Figure 1.5(a).

An example of a raw experimental picture and of a correlation map from the experiment described in section 2.2.1.b are shown on Figure 1.6. On the raw image, the glass beads are

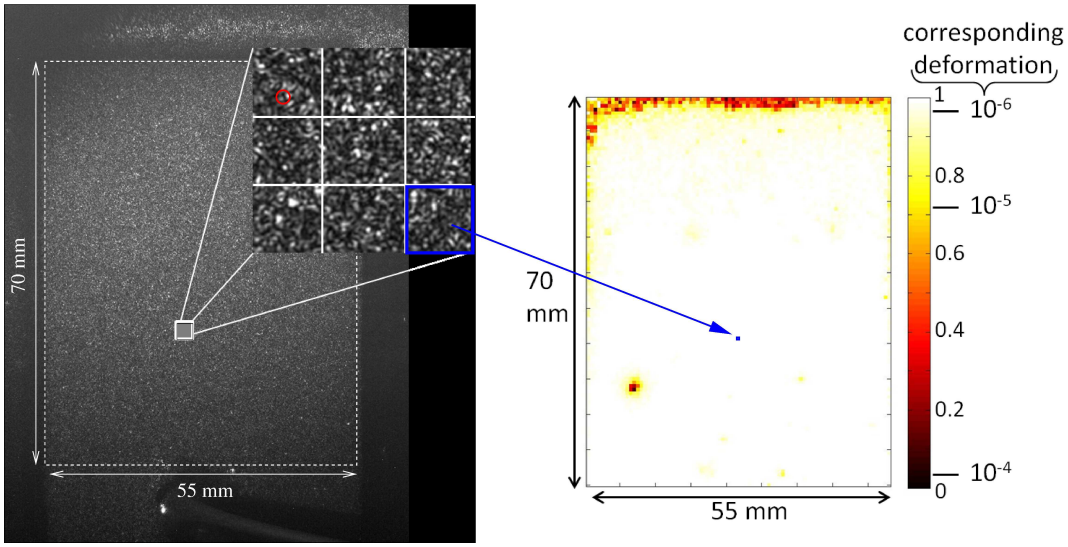

Figure 1.6: Left: raw experimental speckle image (the sample is constituted of glass beads of diameter $d = 90\mu$m, indicated in the inset in red). Right: corrrelation map. Each pixel, as the one colored in blue is obtained from a multispeckle average on small zone from two raw images. The order of magnitude of the deformation indicated on the colorscale is obtained from Equation 1.10.

not visible (a red circle in the inset indicates the size of the glass beads in this experiment), the granular pattern of the image being only due to the speckles. The correlation maps presented in the next chapter will generally have the same kind of colorscale: light color (white or light yellow) corresponds to a correlation close to 1, *i.e.* deformation smaller than 10^{-6}; dark color (black) corresponds to a correlation close to 0, *i.e.* deformation larger than 10^{-4}. The use of this colorscale will always correspond to maps of incremental deformation, *i.e.* correlation calculated between successive speckle images. When the correlation is calculated in reference to a constant image, another colorscale will be used, which will be shown in the next section.

The high sensitivity of the method results in a total loss of correlation for too large deformation. But as in this higher limit classical methods as particle tracking are available, it is possible to shift to more classical method of measurement to follow such deformation. An experiment where the complementarity of DWS and particle tracking is demonstrate can be found in [Crassous et al., 2008].

1.2.3 Validation of the method

We have tested and validated our method by performing experiments in well-controlled configurations of mechanical sollicitation on two kinds of materials [Erpelding et al., 2008, 2013]. Firstly, we used Teflon slabs, which can be considered as perfectly elastic at the deformation of interest in our studies but for which the detailed mechanisms of the scattering process are unknown. Secondly, we used dispersions of 1 μm latex beads in gelatin, which corresponds to Mie scatterers in

an homogeneous matrix but which displays ageing during our experiments so that it was more difficult to procede to "model" mechanical experiments on it.

An exemple of such a test is shown in Figure 1.7. We have applied a ponctual force on a Teflon slab in a plane stress configuration and we have exerted a cyclic force on it. The experimental correlation maps obtained during the cycle are shown on the upper line of Figure 1.7(c). From

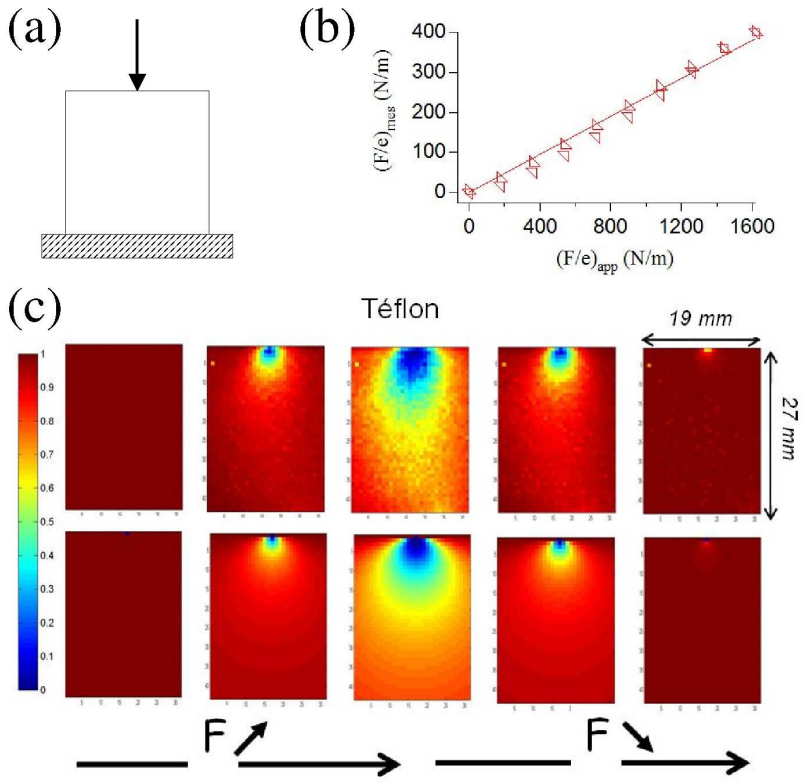

Figure 1.7: (a) Mechanical conditions of loading of the sample. (b) Ratio between the force exerted and the thickness of the sample, as deduced from a fit of the correlation maps $\left(\frac{F}{e}\right)_{mes}$ as a function of the same ratio measured independently $\left(\frac{F}{e}\right)_{app}$. (c) Upper line: maps of correlation during a cyclic charge. Lower line: one-parameter fits of the experimental maps using the analytical model.

the exact solution of elasticity of a ponctual force on an half-infinite plane, we can calculate the analytical form awaited for the spatial dependency of g_I. We can then fit this analytical form to the experimental map with a unique parameter ($\propto c$ coefficient in Equation 1.10). The theoretical maps thus obtained are shown on the lower line of Figure 1.7(c). The comparison between the values of the parameter obtained by the fit ($(F/e)_{mes}$) and the independent measurment of this quantity experimentally ($(F/e)_{app}$) shows that the linearity and reversibility obtained by the local measurement are very good and the order of magnitude of the local measurement correct.

We have extensively discuss the residual discrepancy between the local measurement of the strain and the awaited one in [Erpelding et al., 2008]. We have shown that for a material where the diffusion process is well-known (latex beads in gelatine, *i.e.* Mie scatterers) and when the limited size of the sample is taken into account in the modeling, a good quantitative agreement

is acheived. We are thus very confident in our method, which we have mainly used as a probe of the local deformation and reversibility for the study of the mechanical response of heterogeneous materials, generally without the intent of precise quantitative deformation measurements.

1.3 Other studies concerning scattering

In parallel to the development of the method of measurement of deformation, we have been interested in problematics linked to the propagation of waves in heterogeneous materials and to more fundamental questions linked to scattering.

In the following I will present briefly two studies. In the first one, we consider the possibility to compensate isotropic deformation by changing the wavelength of the light. In this experiment a granular material is used as a scattering media but we will consider it here as an "ideal" heterogeneous material, *i.e.* we will be interested in this section only in questions linked to light propagation, keeping the observations linked to granular materials for the next chapter. The second work presented here concerns the propagation of waves in a chiral scattering.

1.3.1 Wavelength as a tunable parameter

Main associated publication: J. Crassous, M. Erpelding, and A. Amon, ***Phys. Rev. Lett.*** **103**, 013903 **(2009)**.

This particular work had initially a rather fundamental motivation but we will see in the next chapter that it can have in fact very practical application. An interferometric process can be viewed as the measurement of lengths in units of the wavelength of the light probe. If we consider a speckle figure obtained after the propagation of a coherent light through a scattering material, a uniform modification of the paths length in the material should be compensable by a modification of the wavelength (see Fig. 1.8). In spite of the linearity of the Maxwell equations, this result is not trivial as each speckle is the result of the superposition of numerous waves which have followed different paths in the material.

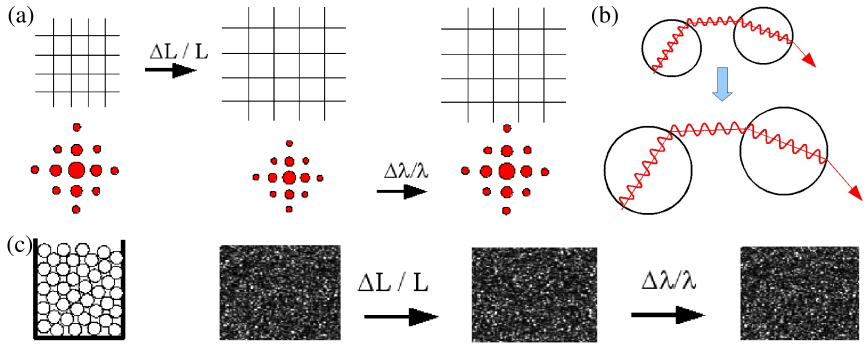

Figure 1.8: Principle of the compensation of an homogeneous deformation by a change of wavelength of the laser source. (a) Simple diffraction: a dilation of a diffraction grid will change homothetically the diffraction pattern. A change of the wavelength of the source allows to recover the initial diffraction pattern. (b) Schematic of the simultaneous dilation of the scatterers (glass beads) and of the wavelength. (c) Principle of our experiment.

We have shown that such an optical compensation of an isotropic deformation of a material is indeed possible when strong scattering is at play. We have used a tunable laser as source and a granular sample submitted to well-controlled thermal expansion to obtain a uniformly deformed material (see Fig. 1.9). The transmitted scattered light is collected in the far field on a CCD camera and the correlation of intensities are calculated over the whole images, as in standard multispeckle methods.

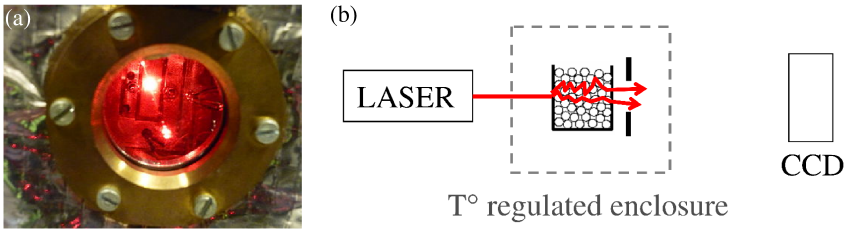

Figure 1.9: (a) Photography of the regulated temperature cell showing the granular sample illuminated by the laser. (b) Schematic of the experiment. The transmitted scattered light is collected on a CCD camera. The ensemble averages for the calculation of the correlation function are obtained using all the pixels of the camera.

As shown in Figure 1.10(a), we were able to recover almost entirely the initial speckle pattern by changing simultaneously the state of deformation of the material and the wavelength of the light probe. The relative wavelength variation and temperature variation at the maximum of recovery of the correlation are proportional (Fig. 1.10(b)), which shows that indeed a wavelength variation is equivalent to a volumic deformation of the scattering material. This affirmation holds in fact whatever the value of the resulting total phase is and not only when the two effects conceled each other. It is what is shown in Figure 1.10(c) where all the values of the correlation measured are represented as a fonction of the relative expansion factor of the optical path: we observe that all the data corresponding to varous temperature and wavelengths collapse then on a unique master curve, which analytical expression can be obtained (blue line in Fig. 1.10(c)).

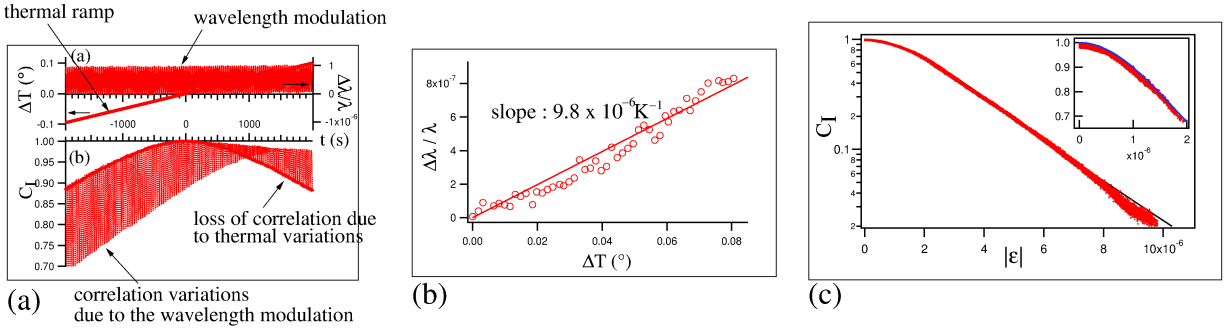

Figure 1.10: (a) Top: temperature variation and modulation of the wavelength of the laser. Bottom: correlation obtained using $t = 0$ s as reference. Thick line: temperature variation alone; Fine line: combination of temperature variation and wavelength modulation. (b) Relationship between the relative wavelength variation and the temperature variation when the maximum of correlation is recovered. (c) Correlation as a function of the relative expansion. Dots: experimental data, blue line: fit from the theoretical expression.

This experiment is not only a beautiful experimental test of some theoretical idea. We will see in the next chapter how it can be used as a tool for the measurement of non-isotropic deformation.

1.3.2 Scattering and chirality

Main associated publication: J. Crassous, A. Amon and J. Crassous, "Circular differential scattering of polarized light by a chiral random medium", ***Phys. Rev. A* 85**, 023806 **(2012)**.

We have studied the differential scattering between left- and right-handed circularly polarized waves propagating in a chiral diffusive material. When this media is almost transparent, we have shown experimentally that the ellipticity of the transmitted wave can be tuned independently from the rotation of the polarization. It is a counterintuitive effect when only the contribution of the differential absorption is considered in the circular dichroism: ellipticity and rotary power are then related by a Kramers-Kronig type relationship and cannot be adjusted independently. We have explained our observation by taking into account the differential scattering contribution in the circular dichroism and we have given a theoretical model and analysis for our experiments in the first Born approximation.

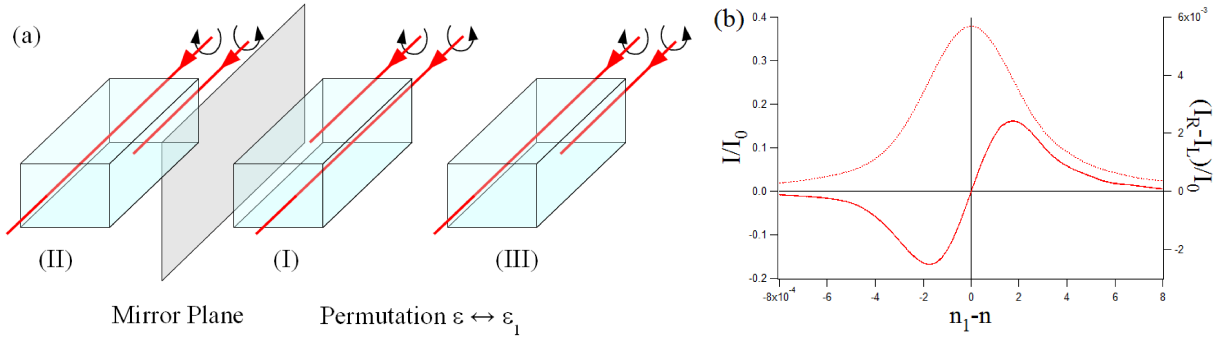

Figure 1.11: (a) Principle of the experiment: a chiral scattering medium differentially transmits right- and left-handed circular waves. If we change the chiral material in (I) by its enantiomer in (II), the difference of transmission between the two opposite circular waves is inverted. If now, keeping the enantiomer (I), we invert the contrast of indices between the two phases that constitutes the heterogeneous material, we can reverse the differential scattering between the two waves. (b) Dotted line, transmission of the scattering material as a function of the refractive index difference between the two phases. Solid line, difference of transmission between left and right circular polarization.

Experimentally, we observe that the difference of scattering cross sections between polarizations of opposite handedness propagating in a dense scattering chiral material can be largely adjusted. Indeed, by tuning the refractive indices of the materials composing the scattering medium around the phase-matching condition, the scattering difference can be varied and even inverted (see Fig. 1.11(b)).

To conclude this chapter, an important part of the research activities of our group in Rennes is related to the propagation of waves in heterogeneous materials. We have demonstrated several

remarkable and elegant effects as the optical compensation of mechanical expansion or the tunability of the differential scattering of circularly polarized waves in materials lacking space-inversion symmetry. In parallel to those fundamental questionning, our works concerning scattering have been motivated by the developpement of a method of measurement of small deformation, with the aim of studying heterogeneous minute deformation in soft matter and disordered materials.

Chapter 2

Plasticity in granular materials

My recent research activities have been mainly devoted to the study of the mechanical behavior of granular materials. Most of the experimental results we have obtained the past few years on this subject have benefited from the use of the method of measurement of small deformation based on DWS exposed in the previous chapter. Such a method has given new insights in the granular matter field because it gives spatially-resolved measurements of strain at a range of deformation (10^{-6} to 10^{-4}) where only scarce information were available before. The spatial resolution of the method (a few sizes of grains) provides a mesoscopic measurement at a scale small enough to understand the local processes at play but large enough to have a continuum mechanics point of view on the system. Because of all those features, the experiments I describe in the following have provided new understanding of elasticity, plasticity and rupture in granular materials.

The chapter is organized as followed. First, a state of the art is given, trying on the one hand to underline the main questions shared by the people working on plasticity of soft glassy material and on the other hand to give briefly some specificities of the mechanical response of granular materials. In a second part, I describe our works on plasticity in granular materials. First I present our studies concerning local rearrangements and their coupling, then I discuss the formation of micro-ruptures in sheared granular materials and finally I expose our works linked to the question of an elastic limit in a granular material. The last part of this chapter is dedicated to my research projects for the next few years.

2.1 State of the art

2.1.1 Disordered materials

Granular matter belongs to the class of soft glassy materials, and shares with those systems several features. They can behave as solids or liquids depending on their loading and they display localization of the deformation. On a general point of view, a whole range of materials (glasses, colloids, foams, granular materials...) shares some properties that are still not well understood, as for example the glass transition, the shear-band formation or the so-called jamming/unjamming transition. Those materials, characterized by their disorder, have common points in their behavior although they are rather different concerning the size of their components and the interactions between the constituants. Nevertheless, as they share several common features, the theoretical

frameworks for their description have numerous overlappings and connections. Among those features are:

- The transition from the unjammed state ("liquid" state) to the jammed state ("solid" state) is not connected to a transition from disorder to order. An amorphous solid is disordered. The definition and identification of that transition are still unclear [Berthier and Biroli, 2009].
- During the transition, the slowing down of the system is not spatially homogeneous. Dynamical heterogeneities are observed linked to collective behavior of the components [Dauchot et al., 2005; Duri and Cipelletti, 2006; Keys et al., 2007].
- Amorphous solids display an excess of low-frequency modes of vibration, the so-called boson peak [Xu et al., 2007].
- When submitted to a deformation, glassy solids tend to display localization of the deformation and exhibits shear bands [Desrues and Viggiani, 2004; Schuh et al., 2007].
- On the side of the unjammed, liquid, state, those materials are complex fluids. Their rheology is often described by a Herschel-Bulkley law. Those threshold fluids exhibit shear bands formation [Schall and van Hecke, 2009].

All those features make the description of these materials difficult. A unified point of view based on a synthetic diagram underlining the universality of a transition between two states, jammed and unjammed, depending on three parameters, temperature, density and load, for a whole class of materials, has been proposed [Liu and Nagel, 1998]. Such a unified point of view motivates to share the tools that have been developped for the understanding of those different materials but the use of the same words to designate analoguous phenomenon have limits. For example, concerning what is called the "jamming transition", the difference between the slowing down of the inner dynamics has to be distinguished from the apparition of the mechanical rigidity in the system [Lechenault et al., 2008]. Another example could be found in the expression "shear bands" which both designates the apparition of a plane of rupture in an amorphous solid and the spatial inhomogeneity of the flow rate in a complex fluid. In the two cases the system indeed exhibits localisation of the deformation or of the strain rate when submitted to an homogeneous stress, but does that mean that there are similarities in the underlying mechanisms at play for the formation of those bands ?

Among the existing frameworks developed for the understanding and description of those systems, we can mention:

- The characterization of the transition point using for example the divergence of the length of the dynamical heterogeneities or the study of the critical slowing down of the dynamics [Berthier and Biroli, 2009].
- The study of the elastic limit of amorphous solids and of the boson peak, including the analysis of the normal modes of the system, their heterogeneities, their destabilization and their link with the non-affine response of the material [Tanguy et al., 2002; Tsamados et al., 2009] as well as the study of the geometrical and isostatic conditions of the jamming transition [Wyart et al., 2005; Van Hecke, 2010].

- The description of the plasticity of amorphous solids based on the existence of "Shear Transformation Zones" where plastic rearrangements take place. Those events can then trigger other rearrangements in a cascade of plastic events which is supposed to lead to shear bands formation [Falk and Langer, 1998; Maloney and Lemaître, 2006].
- Phenomenological models developed for the description of complex fluids, introducing a variable describing the dependency of the viscosity on the ageing and deformation of the system [Sollich et al., 1997; Sollich, 1998; Hébraud and Lequeux, 1998; Derec et al., 2001; Bocquet et al., 2009].

Those different approaches are motivated by the study of specific systems (glass transition, plasticity of metallic glasses, numerical simulation of Lennard-Jones glasses, threshold fluids description...) and address in different ways the same class of problems. Nevertheless the differences between some models are far from obvious. All those questions are actively debated issues and experimental results from diversified systems are crucially needed to go further in the understanding of the elasticity and plasticity of disordered materials.

2.1.2 Elasticity and plasticity of amorphous materials

One of the issue of the description of plasticity in amorphous systems is the fact that the tools that have been developed for crystals are useless. Those theories are based on the existence of defects in regular lattices and plasticity is described in terms of mobility and nucleation of those defects. The intrinsic disorder of amorphous systems prevents to use such an approach. The works of A. S. Argon [Argon, 1979] and F. Spaepen [Spaepen, 1977] for the description of plasticity in metallic glasses introduce a description based on the existence of local plastic events, *i.e.* rearrangements implying a few elements of the system (Fig. 2.1). The sites where those local rearrangements will take place are soft spots of the disordered system. The stress redistribution after such an event can trigger other rearrangements at some other location in the system (see Fig. 2.2). An avalanche-like process can then take place which is supposed to lead to the formation of a shear band.

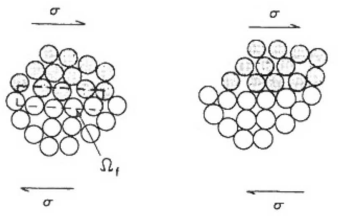

Figure 2.1: From [Argon, 1979]. Schematic representation of a local rearrangement.

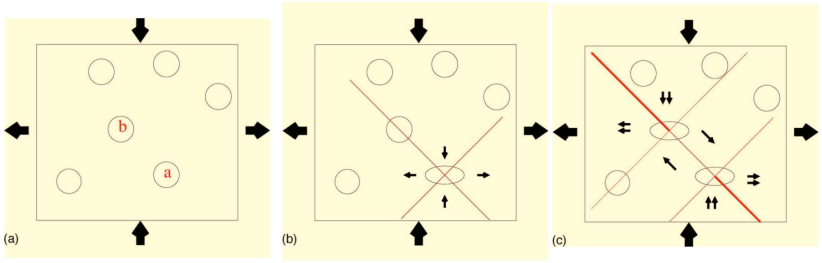

Figure 2.2: From [Maloney and Lemaître, 2006], principle of the avalanche-like process of triggering of rearrangements: the stress field after the change of configuration in ⓐ trigger a rearrangement in ⓑ.

Such plastic rearrangements have been identified in several experimental systems for which the size of the components allows a direct visualization of the events. In foams [Kabla and Debrégeas, 2003], they correspond to T1 event, *i.e.* a change of neighbors between four adjacent bubbles

(Fig. 2.3). In colloidal glasses, they can be visualized using confocal microscopy [Schall et al., 2007] (Fig. 2.4).

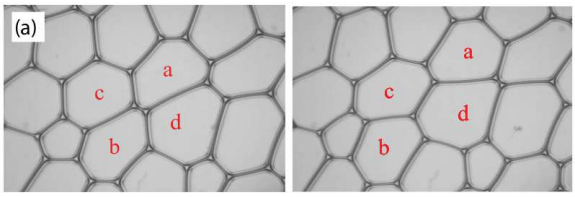

Figure 2.3: From [Kabla et al., 2007], T1 event in a bidimensional foam.

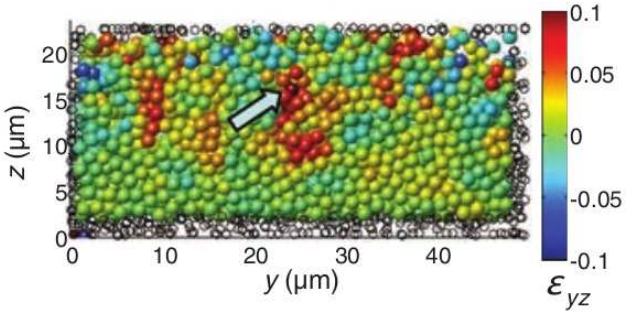

Figure 2.4: From [Schall et al., 2007], local plastic rearrangement in a colloidal glass.

On the numerical side, simulations of several types of amorphous materials have studied such local rearrangements, as, for example, in bidimensional foams [Kabla and Debrégeas, 2003] or Lennard-Jones glasses [Falk and Langer, 1998; Maloney and Lemaître, 2006; Tanguy et al., 2006; Tsamados et al., 2008]. The stress redistribution generated by an event (see Fig. 2.5 and 2.6) has been studied, showing its quadrupolar nature. Avalanche-like processes forming transient slip lines have been evidenced [Maloney and Lemaître, 2006]. Such transient micro-bands have also been observed in numerical simulation of frictional granular materials [Kuhn, 1999], but their link with the final, permanent shear-band is still not well understood [Gimbert et al., 2013].

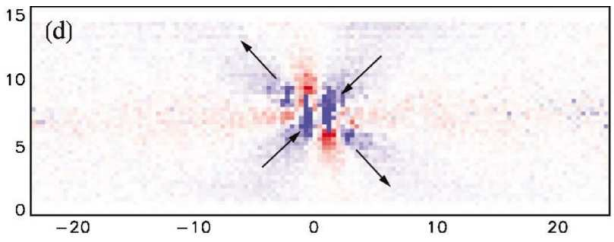

Figure 2.5: From [Kabla and Debrégeas, 2003], stress redistribution after a T1 event in a simulation of a bidimensional foam.

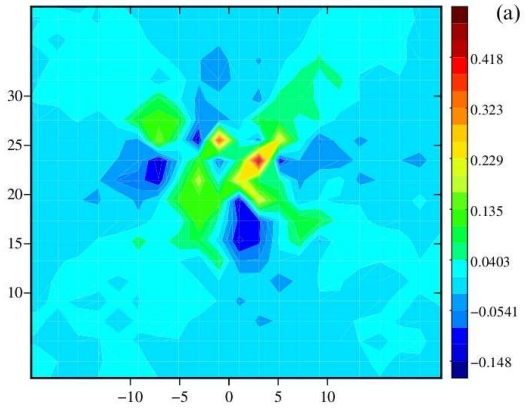

Figure 2.6: From [Tsamados et al., 2008], stress field associated to a local rearrangement in a Lennard-Jones glass.

On the theoretical side, the description of the plasticity in amorphous materials often relies on an energy landscape point of view [Sollich et al., 1997; Falk and Langer, 1998] in which a jump of a potential barrier corresponds to a local rearrangement. In those mean-fields models, the stress redistribution in the disordered system after a platic event is described as a mean mechanical noise. The activation of the barrier jump leads to the introduction of an effective temperature, which

can be indeed the temperature of the system, but can also describe the previously mentioned mechanical noise [Sollich et al., 1997] (especially in the case of athermal systems as granular media) or be linked to the local configuration, through for example the local free volume [Falk and Langer, 1998]. Those models have similar basis but I will separate two approaches in the following that I understand as being motivated by a point of view on the system as being either more "solid" or more "liquid".

In the case of the "Shear Transformation Zones" theories (STZ) [Falk and Langer, 1998; Bouchbinder et al., 2007], models are based on the pre-existence of a scarce population of spots, the STZ, included in an otherwise elastic medium. In the simplest point of view, those STZ corresponds to bistable sites which can take two configurations depending on the direction of the shear. Such feature leads to two characteristics: reversibility when the shear is reversed in direction and saturation after their commutation in the direction of the shear.

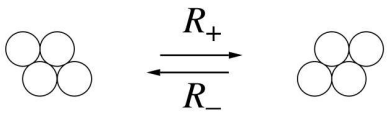

Figure 2.7: From [Lemaître, 2002], schematic representation of a reversible STZ.

Those models lead to kinetic equations for the density of the two types of configuration of STZ, including the creation and annihilation of zones during the loading of the material. The activation of the defects is described by a term including an effective temperature which is linked in [Falk and Langer, 1998] to the excess of local free volume. Such hypothesis imply a possibility to identify experimentally the location where the STZ should take place. Such measures are for example possible in colloidal glasses using confocal microscopy. Yet, no conclusive experimental link between the local structure of the material (free volume, number of contacts...) and the location of the rearrangements has been given for the moment [Manning and Liu, 2011].

Going towards the elastic limit, several works have tackled the issue of the specificities of the elastic response of amorphous solids because of their intrinsic disorder: the validity of the definition of elasticity in a continuum mechanics point of view depending on the coarse-graining used to describe the system [Goldhirsch and Goldenberg, 2002; Tsamados et al., 2009], and its link with the non-affine response of disordered materials [Barrat, 2006] (see Fig. 2.8). Works based on numerical simulations of Lennard-Jones glasses [Tanguy et al., 2002; Tsamados et al., 2009] have shown that it was possible to define a Hooke law from a characteristic size of several diameters of grains for the coarse-graining scale. The map of the local elastic moduli is heterogeneous (Fig. 2.9) and soft spots can be identified where the local rearrangements are expected to happen. The observed non-affine displacement for very small deformation is link to the local value of the elastic modulus and displays vortex figures showing concentration of displacement (Fig. 2.9) [Radjai and Roux, 2002]. Numerical simulations on discs interacting through Hertz potential [Manning and Liu, 2011] confirm that the identification of the most unstable elastic modes, of quasi-localized structure, are good candidates for the experimental identification of the potential zones of rearrangements. Those results pave the way for an experimental recognition of the soft spots in the materials before their failure but a clear picture is still missing [Tan et al., 2012; Chen et al., 2011].

Another class of models are gathered under the terminology of "Soft Glassy Rheology" (SGR) [Sollich et al., 1997; Sollich, 1998; Hébraud and Lequeux, 1998]. Those theories are motivated by the description of the rheology of complex fluids. In the energetic landscape description, mesoscopic elements are considered in order to describe a cage dynamics [Sollich et al., 1997], the jump of a

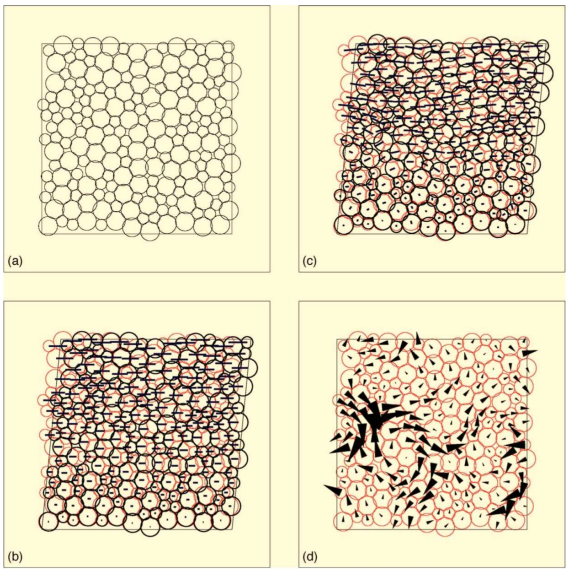

Figure 2.8: From [Maloney and Lemaître, 2006], non-affine response in a disordered system. (a) to (b): an homogeneous shear is applied to an ensemble of particle, but in (b) the particles are then not in mechanical equilibrium. The mechanical equilibrium is obtained through correction in (c). The difference between (c) and (b) gives the non-affine field of displacement (d).

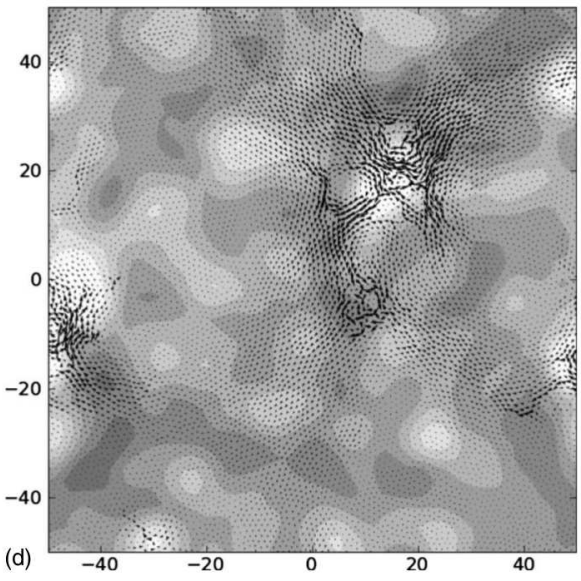

Figure 2.9: From [Tsamados et al., 2009], in gray levels: map of the local shear moduli, (stiff: black; soft: white). Arrows: non-affine displacement.

potential barrier corresponding to a local rearrangement. Equations in that class of models are expressed in terms of probability distribution in the energetic landscape. Bistability and saturation of the mesoscopic elements are not considered: in a fluid-like point of view, when a particle has jumped outside a cage, it can not come back to the initial cage when the shear is reversed.

In the continuation of the SGR point of view, a more phenomenological approach considers constitutive equations for the stress and a phenomenological variable called "fluidity" [Derec et al., 2001]. That fluidity corresponds to the rate of relaxation of the stress and is considered as dependent on the ageing of the system and of the rejuvenation generated by the deformation. While the previously mentioned mean-field theories do not include explicitly the spatial coupling between the rearrangements, several fluidity models include a non-local term with a correlation length in their equations [Picard et al., 2005; Bocquet et al., 2009; Kamrin and Koval, 2012]. The requirement of such a nonlocal law has been demonstrated through the analysis of experiments of confined flows of concentrated emulsion displaying cooperativity in the flow [Goyon et al., 2008].

I have attempted to give a broad picture of different models aiming at the description of amorphous glassy systems which will be used in the following for the understanding and the modeling of our experiments. As the experiments I will discussed here have been conducted on granular materials, I will end this state of the art by some aspects specific to granular materials.

2.1.3 Granular materials: common points and specificities

As amorphous materials, dry granular media have specificities such as [Andreotti et al., 2012]:

- Granular materials are athermal. As will be seen in the following, it rises some questions when using SGR models to describe creep processes in granular media [Nguyen et al., 2011].
- The preparation of a granular system before an experiment is crucial. The observed behavior is dependent on the preparation, which can lead to a texture in the pile [Vanel et al., 1999; Atman et al., 2005].
- The local description of the interactions between the grains have several specificities linked to the frictional contact. In the absence of cohesion, the local tensile force is null while the compressive force is large (hard spheres) and describe by a nonlinear, hertzian, contact. The local shear can be described by a local Coulomb friction law.
- Because of the nature of those interactions, stress transmission in a granular packing is inhomogeneous and imply a network of contact called force chains [Liu et al., 1995; Radjai et al., 1996; Majmudar and Behringer, 2005].

I will now focus on some aspects of the behavior of a granular sample quasi-statically loaded until failure.

2.1.3.a Elastic limit

Because of the nature of the interaction between grains, the existence of a domain of elastic response for a granular material may be questioned: even for very small deformation, some local irreversible rearrangements take place [Divoux et al., 2008; Divoux, 2009] and because of force chains, a small localized rearragement can lead to a collapse of a part of the force network [Cates et al., 1998].

From a theoretical point of view, the equations giving the response of granular materials in an elastic limit is a debated issue [Herrmann et al., 1998]. In the soil mechanics community, models coming from continuum mechanics as elasto-plasticity [Nedderman, 2005] are used to describe the response of a granular pile. A part of the physicists community has questioned the validity of the use of such elliptics equation and have proposed other models taking into account the existence of force chains for the stress repartition [Bouchaud et al., 1995; Coppersmith et al., 1996]. Yet, when some features as disorder [Bouchaud et al., 2001] or as the lengthscale at which the system is probed [Goldenberg and Goldhirsch, 2005], are taken into account, the difference between those points of view become unclear. The experimental investigations done by G. Reydellet [Reydellet, 2002] during is PhD on tridimensional [Reydellet and Clément, 2001] and bidimensional [Geng et al., 2001] packings have shown that the spatial response of the system to a ponctual force can be interpreted in the framework of anisotropic elasticity.

Another class of experimental works that have shown that elasticity (possibly anisotropic and nonlinear) can be used to describe a granular material at very small deformation are acoustical measurements, which have shown that an effective medium point of view is relevant [Jia et al., 1999; Makse et al., 2004; Somfai et al., 2005]. Yet, when the confinment is weak, especially near the free surface, the existence and definition of an elastic response is still problematic [Bonneau et al., 2008].

2.1.3.b Elasto-plasticity and failure criteria

When considering the loading of a granular material, the simpliest description of the behavior is an elasto-plastic model (see Fig. 2.10). A criterion is then needed to predict the critical stress σ_c at which the failure occurs. The most known and used is the Mohr-Coulomb criterion which gives a threshold value as a function of an internal friction $\mu = \tan\phi$ of the material and predict the inclination of the slipping planes [Nedderman, 2005]. When an angle θ exists for which the ratio of the shear stress and normal stress τ_f/σ_f reaches μ, the material breaks along the plane determined by θ (see Fig. 2.11). Most of the studies in soil mechanics are done in biaxial configuration (see Fig. 2.11) where two principal stresses are imposed on the material. In those kind of experiments, the relevant stress for the stress-strain curve is then the difference $\sigma_1 - \sigma_3$, which is usually called deviatoric stress, and the relevant deformation is the axial strain. The Mohr-Coulomb failure occurs when $\frac{\sigma_1-\sigma_3}{\sigma_1+\sigma_3} = \sin\phi$ and the angle of failure is given by $\theta_f = \frac{\pi}{4} + \frac{\phi}{2}$.

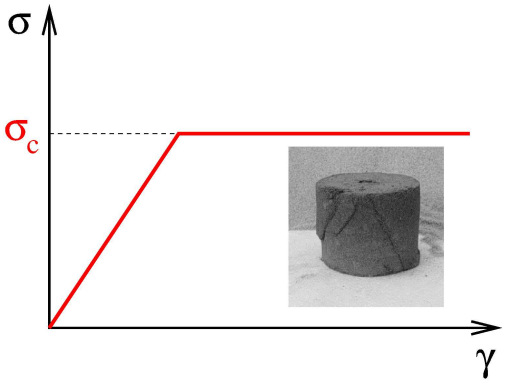

Figure 2.10: Ideal response of an elasto-plastic solid, σ is the stress applied to the system and γ its deformation. Inset: figure from [Desrues and Chambon, 2002], sample after failure showing shear planes.

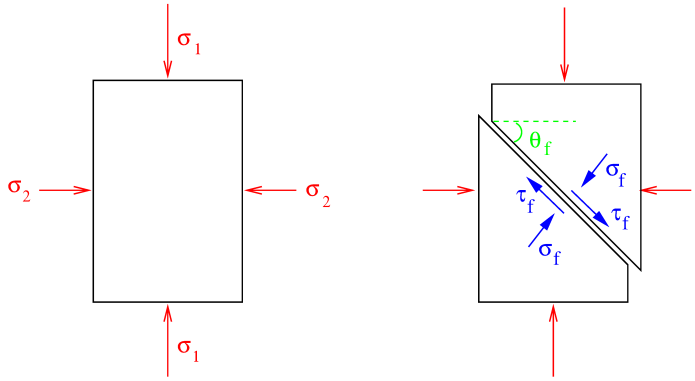

Figure 2.11: Left: principle of a biaxial test. Right: Mohr-Coulomb failure.

If a lot of experiments are in agreement with this theory, other angles of shear planes are also observed in soil mechanics loading tests [Bésuelle and Rudnicki, 2004; Hall et al., 2010], and other predictions for the angle of the failure plane exists [Bésuelle and Rudnicki, 2004]. In particular, K. H. Roscoe [Roscoe, 1970] proposed that the planes of failure in some geometries of loading will correspond to zero extension lines of the deformation, giving a predicted angle generally smaller than the Mohr-Coulomb one. Ultimately, the observed angle in a given experiment is always justified *a posteriori*, and, as the same apparatus can lead to the observation of different angles [Hall et al., 2010], the situation remains rather unclear. Finally, other modes of rupture exists in the materials, as diffuse modes of rupture [Desrues and Georgopoulos, 2006] and transient modes of localization [Hall et al., 2010].

2.1.3.c Critical state theory

In the previously described elasto-plastic model, no plasticity is considered in the granular material before the failure. Yet, the description of the change of volumic fraction during a test leads to

the necessity to describe the *yield* process, *i.e.* the plastic deformation that occurs inside the sample before the failure. The critical state theory [Schofield, 1968] is based on the experimental observation that loose and compacted samples both converges to a similar state, called the *critical state*, at the end of a test (see Fig. 2.12). The final volumic fraction converges at the end of a test towards a value which is independent of the preparation of the sample. However, it has to be underlined that the measurements underlying this theory are global, averaged on the whole sample, while the final localization of the deformation leads to large heterogeneities of volumic fraction in the sample.

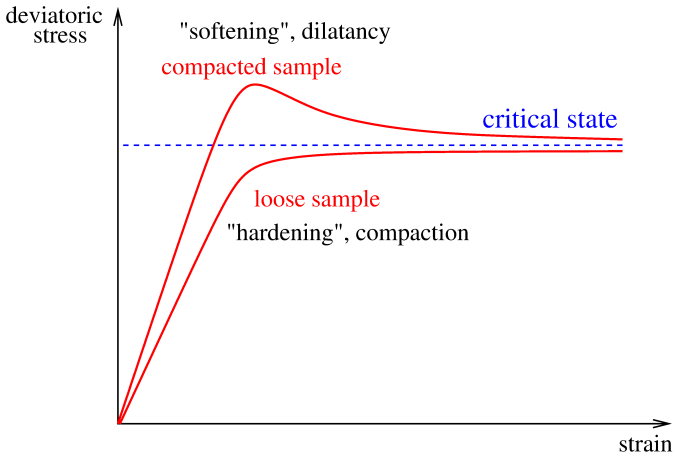

Figure 2.12: Schematic mechanical response of respectively a loose granular sample and a compacted one submitted to a biaxial test.

Specifically in the critical state theory, when the granular material is initially dense, the picture coming from elasto-plasticity is still valid: the response of the system is elastic until failure, after which dilatancy occurs. If the granular material is initially loose, an elastic response is still awaited at first, but there will be a plastic behavior between the end of the elastic response and the failure: some plastic deformation corresponding to a slow compaction of the sample occurs until a threshold depending on the confining pressure. At this threshold failure of the sample occurs.

The recent progresses in full-field measurements and X-ray tomography [Viggiani and Hall, 2004] is leading to a growingly detailed description of all those processes, with the hope to a progressive connection between micro-mechanical descriptions [Rechenmacher, 2006; Tordesillas, 2007] and continumm mechanics models. In this context, our works on granular materials are a physicists approach for the understanding of the basic mechanisms at the heart of the processes previously described.

I have presented here several theories and frameworks without aiming at a comprehensive review but trying to give the main models that will be used in the following to interpret our observations on granular materials. The principal results from those experiments are detailed in

the next section. We will see that the picture of local rearrangments and their coupling is indeed accurate to understand and describe the plasticity of granular material but that the process of formation of ruptures still need to be understood.

2.2 Mechanical response of granular materials

In this section, I expose our works of the past few years concerning the mechanical response of granular materials. The experimental configurations I will discuss in the following are gathered in Figure 2.13. Those studies are the result of a joint work between J. Crassous and myself and imply several collaborators as explained in each sections. The two first set-ups have allowed us to visualize the localized rearrangements at the origin of plasticity in granular materials. In particular, with the biaxial test, we have evidenced the coupling between the rearrangements and the structuration of the plastic flow during the yield process. Those two experiments are the subjects of the subsection 2.2.1. The formation of the final shear-band is still largely a work-in-progress, yet we have studied micro-ruptures formation during a loading process. I detail in subsection 2.2.2 those experimental studies of micro-ruptures formation in different configuration and chiefly in the case of the tilted box. Finally, I will expose in the last subsection 2.2.3 our works linked to the question of the elastic response of granular materials through two set-ups: thermal expansion and cyclic localized force.

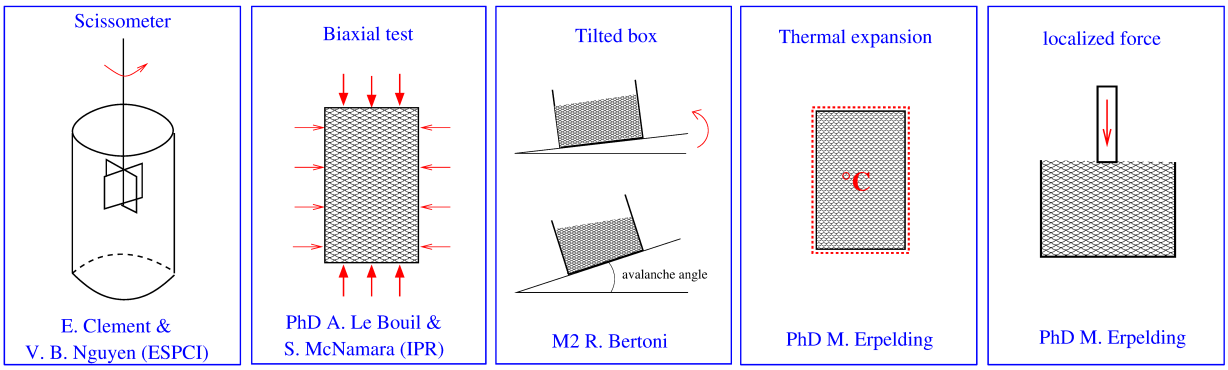

Figure 2.13: Experimental set-ups studied and main collaborators.

In all those experiments, the granular material consists of monodisperse glass beads. The diameter d of the beads used in the various experiments is in the range 100 μm to 500 μm. Piles of such grains strongly scatter light in the visible range and are consequently typically the kind of materials on which the method of measurement of minute deformation presented in the previous chapter can be used. For some of the set-ups we also did experiments with white sand, for which our method is still accurate if the absorption is small enough [Amon et al., 2013]. The details of the optical set-ups and of the obtention of the deformation maps are not recalled as the general principle has been already described in section 1.2. Except in the case of the experimental results presented in subsection 2.2.3, all the deformation maps are incremental, *i.e.* they correspond to correlation calculated between consecutive speckle images, with a colorscale where the darkest

color correspond to large deformation and the lighter color to small deformation.

2.2.1 Plastic flow in a granular sample at small deformation

2.2.1.a Local plastic events

Main associated publication: A. Amon, V. B. Nguyen, A. Bruand, J. Crassous and E. Clément, ***Phys. Rev. Lett.*** **108**, 135502 **(2012)**.

The confrontation at the local scale between theories coming from soft glassy models and the behavior of a real granular material has first been done during a collaboration with E. Clément (PMMH, ESPCI, Paris) during the PhD of V. B. Nguyen (PMMH, ESPCI, Paris). They developed in their laboratory a well-controlled rheometer where the global measurements available are the torque exerted on the rotating vane immersed in the granular material and the rotation of that vane (see Fig. 2.14). They studied the response of the system at imposed stress and imposed strain rate [Nguyen et al., 2011]. In the case of stress imposed experiments, they evidenced a creep process that they have interpreted in the framework of a model from Soft Glassy Rheology [Derec et al., 2001]. A local measurement of the deformation in the sample was lacking to fully understand and interpret the global mechanical response of the system. Our interferometric measurements allowed us to identify localized rearrangements during the deformation of the sample.

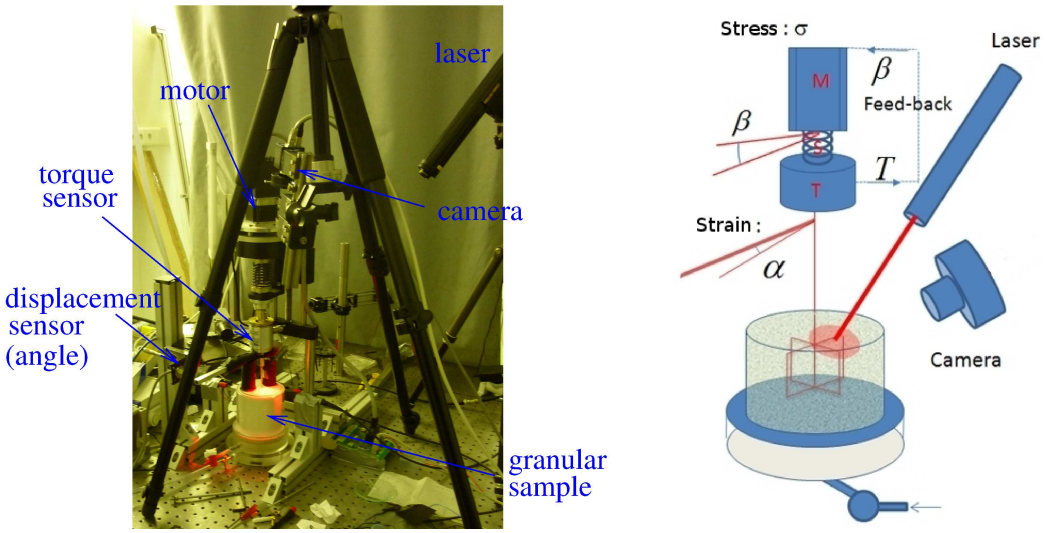

Figure 2.14: Experimental setup. The shear cell is a scissometer, *i.e.* a four-blade vane inserted in a granular material (glass beads, diameter 200 μm). The granular material is carefully prepared at controlled volumic fraction using a fluidization device which is shut down during the mechanical test. The cell can be used either at imposed rotation rate or at imposed shear stress. The vizualisation device, here on two tripods (one for the laser, the other one for the camera and its optics), is now installed on permanent structures.

We have evidenced plastic events which have a typical size of ten grains and a duration of typically less than the inverse of the frame rate, 1 s, *i.e.* they ususally are observed only on one correlation map (see Fig. 2.15). Those spots have been seen in the strain imposed and in the stress imposed experiments. To understand the link between those local rearragnements and

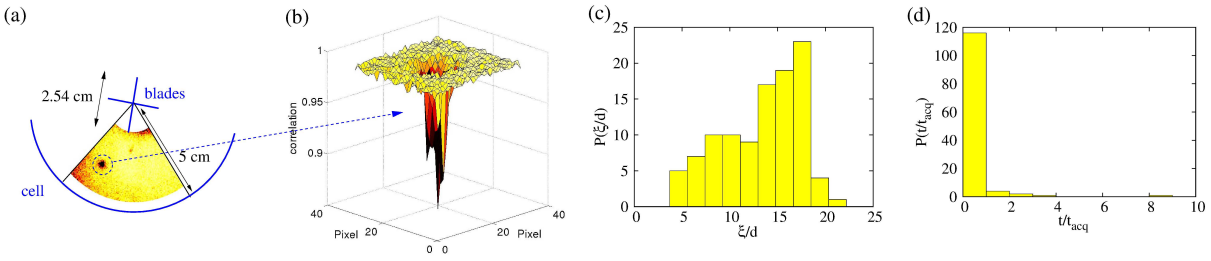

Figure 2.15: (a) Correlation map obtained from imaging the top of the shear cell showing a local rearrangement (light yellow: correlation close to 1 (no deformation), black: correlation smaller than 0.95). (b) 3-D representation of the correlation at the spot location. (c) Size distribution of the spots in units of bead diameter. (d) Histogram of spots duration in units of the inverse frame rate.

the macroscopic deformation we have studied in detail the stress imposed experiments and the relationship between the observed macroscopic creep and the local deformation. The results of that comparison are gathered in Figure 2.16(a). Blue triangles correspond to the macroscopic measurement of the deformation through the slow rotation of the vane when a shear stress is imposed. The blue line is a fit based on a model coming from a SGR model [Derec et al., 2001]:

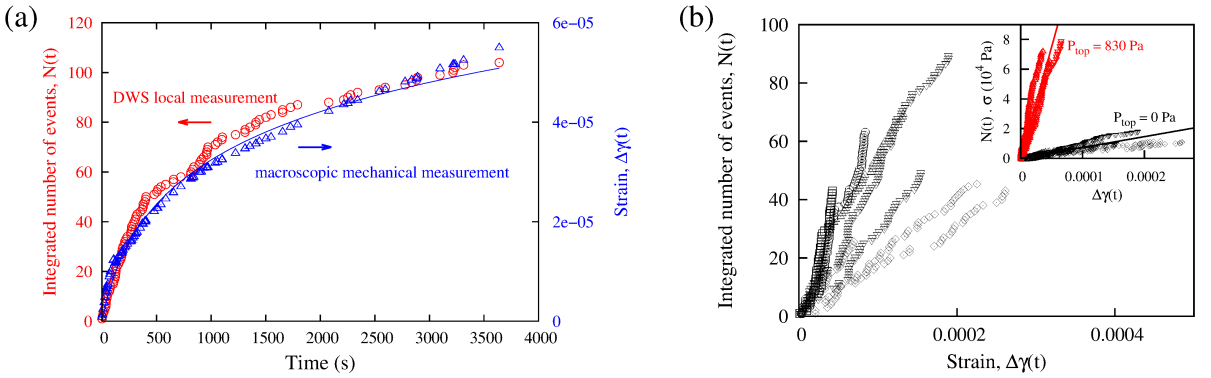

Figure 2.16: Stress imposed experiments. (a) Comparison of global measurement of the deformation based on the rotation of the vane (blue triangles) and of the number of spots that have appeared since the beginning of the creep process (red circle). (b) Number of spots N in function of $\Delta\gamma$ for different values of σ. Insert: σN in function of $\Delta\gamma$ for two values of the shear modulus G.

$$\begin{aligned} \frac{\partial \sigma}{\partial t} &= -f\sigma + G\dot{\gamma} \\ \frac{\partial f}{\partial t} &= -af^2 + r\dot{\gamma}^2 \end{aligned}$$

where f is a phenomenological variable called fluidity which characterizes the stress relaxation rate and G is the shear modulus (measured independantly in the experiment). The difference with a Maxwell model [Oswald, 2005] comes from the phenomenological equation on f which includes ageing ($-af^2$), and rejuvenation caused by the shear rate ($r\dot{\gamma}^2$). For stress imposed conditions,

the awaited behavior for the shear rate is then:

$$\frac{1}{\dot{\gamma}} - \frac{1}{\dot{\gamma}_0} = \frac{G}{\sigma} a_{eq} t \tag{2.1}$$

where $\dot{\gamma}_0$ and a_{eq} are fitting parameter. This expression leads to the logarithmic curve in Figure 2.16.

The red dots in Figure 2.16(a) correspond to the counting of spots during the creep process. We observe a proportionality between the accumulation of the local spots and the global deformation. Such a proportionality can be interpreted in the framework of the SGR model by supposing that the phenomenological variable f corresponds experimentally to the occurence rate of the local events. That assumption leads to the following relationship:

$$G\Delta\gamma(t) \propto \sigma N(t) \tag{2.2}$$

The study of that proportional relationship can be done by studying the evolution of the global deformation $\Delta\gamma$ with the number of spots N for different values of the imposed stress σ and of the shear modulus G as shown on Figure 2.16(b).

The fact that there is a correlation between the number of spots and the global deformation does not prove that the global deformation is the result of the accumulation of the spots. We have thus calculated the energy released by a spot using the measurement of the local strain obtained by the optical measurement. Supposing that the density of spots is uniform in the system, we have shown that the total energy released by all the spots is indeed of the order magnitude of the total work done by the vane during the creep process.

As we have seen in the previous section, such local plastic events are at the basis of several theories describing plasticity in amorphous materials (see section 2.1.2). In those theories, the stress redistribution induces by one event can trigger other rearrangements and a cascade of such events is supposed to lead to the formation of shear bands. I present in the following recent results evidencing such coupling but showing that this scenario is not sufficient to explain the final shear band formation.

2.2.1.b Coupling between the local rearrangements

Main associated publications:

- A. Le Bouil, A. Amon, S. McNamara, and J. Crassous, ***submitted to Phys. Rev. Lett.***
- A. Le Bouil, A. Amon, J.-C. Sangleboeuf, H. Orain, P. Bésuelle, G. Viggiani, P. Chasle, and J. Crassous, ***Gran. Matt.*** **16**, 1 **(2014)**.

In the study we have done in collaboration with E. Clément and V. B. Nguyen, we observed in strain rate imposed experiments, avalanche-like behavior of local events correlated to micro-ruptures observed on the stress curve (see Fig. 2.17). Those observations are in agreement with the scenario of a cascade of local rearrangements leading to shear band formation. Nevertheless, the small size of the region of interest of that study prevented a quantitative study of the spatio-temporal correlations between the spots.

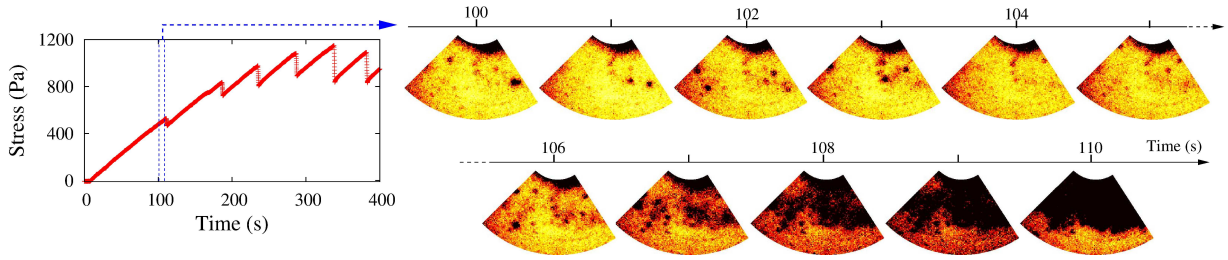

Figure 2.17: From [Amon et al., 2012]. Strain rate imposed experiment in the shear cell of Figure 2.14. Left: loading curve. The rotation rate is of the order of 10^{-3} rad.s^{-1}. Right: successive correlation maps showing the accumulation of spots building up in a micro-rupture. The most decorrelated map correspond to the stress drop on the loading curve.

We were able to complete such an analysis using a biaxial setup we have built in Rennes during the PhD thesis of Antoine Le Bouil [Le Bouil et al., 2014b] and shown on Figure 2.18. The conception of this device has been made in collaboration with P. Bésuelle and C. Viggiani (L3S-R, UJF, Grenoble) and H. Orain and J.-C. Sangleboeuf (IPR, Université Rennes 1). The mechanical configuration corresponds to a standard plane-strain biaxial setup: the two principal stresses in the plane of visualization are controlled while displacements in the orthogonal direction are impeded by solid walls. The stress σ_{xx} (see Fig. 2.18(c)) is imposed by a controlled depressurization of the sample while in the other direction a quasi-static displacement is imposed (1μm/s) and σ_{yy} deduced from the measurements.

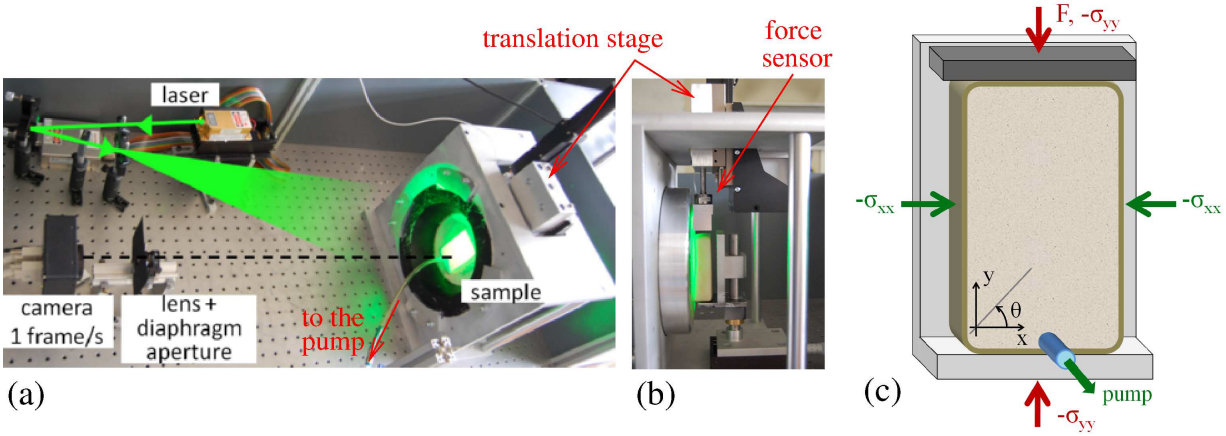

Figure 2.18: (a) Photograph of the optical setup seen from above. (b) Side photograph of the biaxial test. (c) Schematic of the mechanical conditions imposed to the sample. At the front of the sample, the glass window through which the observation is done is not represented.

During the loading of the sample, we observe successively three typical behavior shown in Fig. 2.19(a). First, we observe isolated events of the same type as the ones which have been described in the previous section. Then we observe a structuration of the flow which take the form of transient micro-bands, and finally, two permanent shear bands are visible after the failure of the sample. The nature of the micro-bands on the one hand and of the final shear bands on the

second hand is very different. Firstly, the micro-bands are transient while the final shear bands are persistent, secondly, their respective angles of inclination are clearly different.

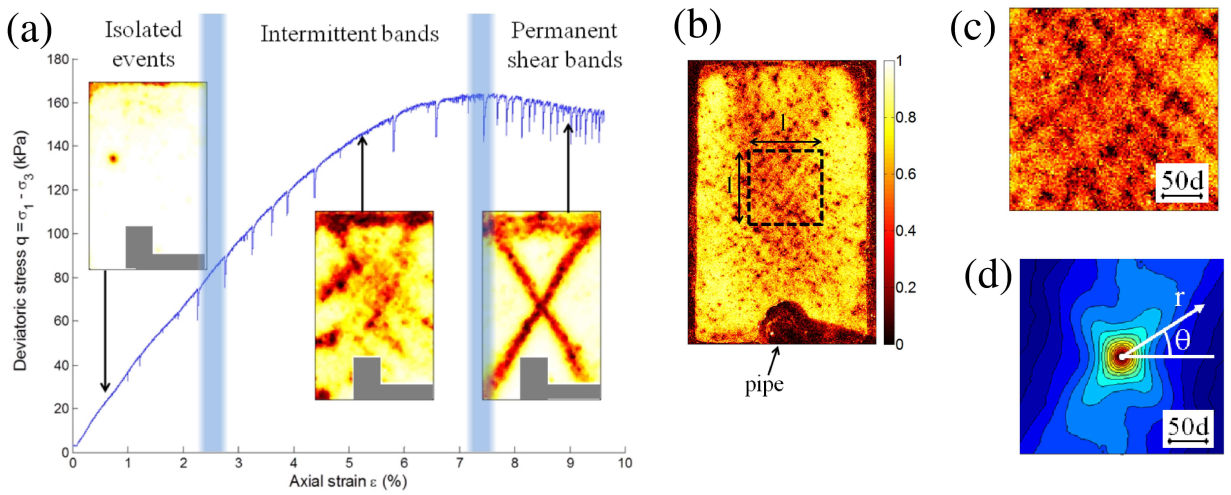

Figure 2.19: (a) Stress-strain curve during a biaxial test. Insets: three typical correlation maps corresponding to the three stages of the deformation. (b) A correlation map showing micro-bands and the region of interest for the quantitative study. The incremental axial deformation between the speckle images is $\sim 3\times10^{-5}$. The difference in resolution between the maps in (a) and this one has been obtained by using a camera with better resolution (number of pixels $\times 9$). (c) Region of interest. (d) Spatial correlation of the map of correlation (c) after averaging.

To characterize quantitatively the micro-bands, we calculate the spatial correlation on a central square part of the correlation maps far from the boundaries of the system as indicated on Figure 2.19(b) and (c). A spatial correlation $\Psi(\epsilon, r, \theta)$ for $\epsilon = 3.30\%$ is shown on Figure 2.19(d), after averaging over 100 map, *i.e.* for a cumulated $\delta\epsilon = 3.2 \times 10^{-3}$. The evolution of this spatial correlation during the loading is shown on Figure 2.20(a). We see that very early in the loading curve, correlation along two symetrical directions appear, given by $\theta_E \simeq 53°$. This direction is almost constant during the loading and clearly different from the angle of the final permanent shear bands ($\theta_{MC} \simeq 66°$).

If the direction does not vary, the length of correlation along the directions $\pm\theta_E$ increases on average during the loading. To measure that length and to obtain its dependence with the deformation, we extract the profile of the correlation along those preferential directions. More precisely, we calculate the *anisotropic part* of the spatial correlation along the directions $\pm\theta_E$:

$$\chi(\epsilon, r) = \frac{1}{2}[\Psi(\epsilon, r, \theta_E) + \Psi(\epsilon, r, -\theta_E)] - \frac{1}{2\pi}\int_0^{2\pi} \Psi(\epsilon, r, \theta)d\theta \tag{2.3}$$

The functions $\chi(\epsilon, r)$ are plotted in function of r/d for different values of ϵ on Figure 2.20(c). The position ξ of the maximum of each curve, obtained by a quadratic fit, are calculated. The values of ξ/d as a function of the axial deformation ϵ are the red squares in Figure 2.20(d). We observe that this length increases until the rupture indicated by the vertical dashed line. We have also studied the persistence of those structures and have shown that this persistence tends also to increase when going closer to the failure [Le Bouil et al., 2014a].

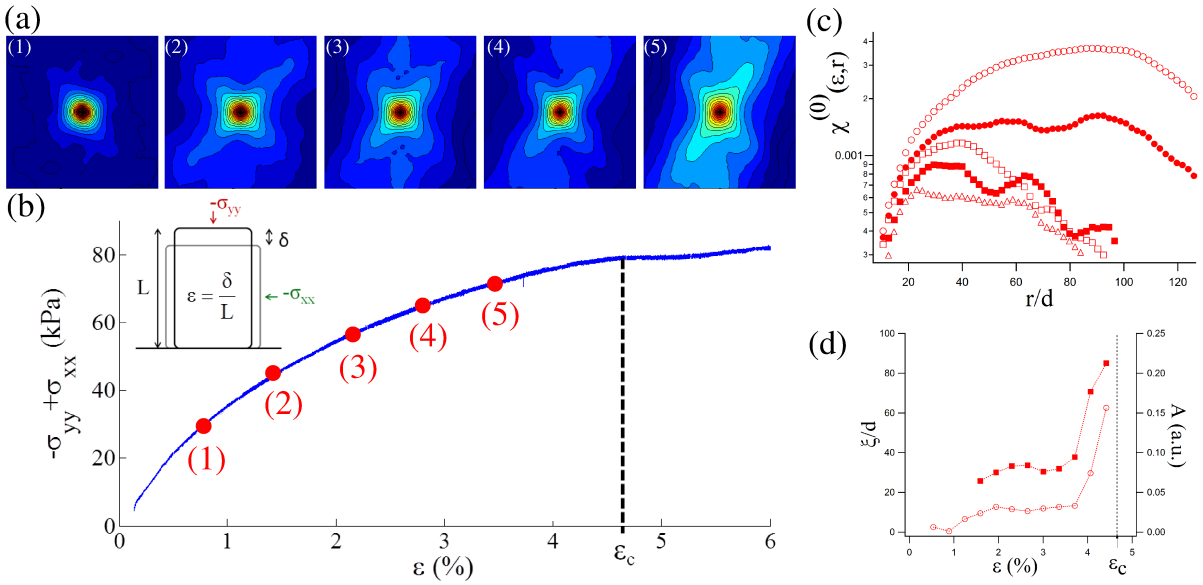

Figure 2.20: (a) Spatial correlations of the maps of deformation for increasing axial strain ϵ. (b) Stress-strain curve indicating the deformation of the sample for each of the spatial correlations of (a). ϵ_c indicates the rupture. (c) Anisotropic part of the spatial correlation along the preferential directions as a function of r/d for different values of the axial strain ϵ. (d) Position ξ/d of the maxima of fits of the curves shown in (c) and area A under those curves as a function of ϵ.

To understand the orientation of those micro-bands, which is clearly different from the Mohr-Coulomb angle, we have built on the models exposed in the state of the art (section 2.1.2). We consider that the material surrounding an isolated rearrangement can be considered as elastic (see Fig. 2.21(a)). We can then solve analytically the problem of an inclusion experiencing a plastic deformation in an homogeneous material [Eshelby, 1957]. The calculation of the deviatoric stress $\tilde{\sigma}_{xx} - \tilde{\sigma}_{yy}$ induced in the elastic surrounding medium because of the isolated rearrangement is proportional to:

$$f(\theta) = (e^*_{xx} - e^*_{yy}) \left[-\frac{15}{4}\cos(4\theta) + \frac{8\nu - 7}{4} \right] - \frac{9}{2}(e^*_{xx} + e^*_{yy})\cos(2\theta),$$

where e^*_{xx} and e^*_{yy} are the only non-null components of the strain tensor characterizing the plastic event and ν is the Poisson ratio of the elastic matrix.

If $\tilde{\sigma}_{xx} - \tilde{\sigma}_{yy} > 0$, the redistributed stress adds to the applied one (see Fig. 2.21(b)), increasing the strain in those direction. When the transformation is isovolumic, those directions are $\theta^*_E = \pm\pi/4$ (case of Fig. 2.21(b)), while, for the geometry of our experiment, θ^*_E increases (resp. decreases) for a dilating (resp. contracting) rearrangement, with a largest value of 54°, which is close to the measured direction of the micro-bands in our experiment.

In parallel to the experiments and to the analytical calculation, Sean McNamara (IPR, Rennes) has performed numerical bidimensional Discrete Element Method simulations of a bi-axial compression test using a visualization method inspired by the experimental technique (see Fig. 2.21(c)). His simulations has shown that the quadrupolar structure of the reorganizations

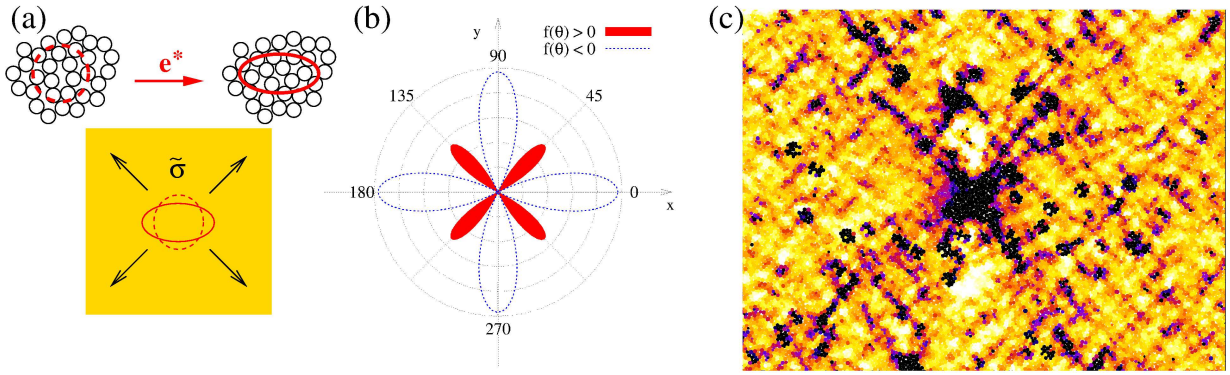

Figure 2.21: (a) Schematic representation of a local plastic event. $\mathbf{e}^*$ is the strain characterizing the plastic transformation and $\tilde{\sigma}$ the stress redistributed in the elastic surrounding because of this plastic transformation. (b) Angular distribution of $\tilde{\sigma}_{xx} - \tilde{\sigma}_{yy} \propto f(\theta)$. (c) Example of a deformation map from a DEM simulation displaying a local event and micro-bands.

evidenced in numerical simulation of numerous systems interacting with various potentials [Maloney and Lemaître, 2006; Kabla et al., 2007; Tsamados et al., 2008] still hold in the case of frictional contact. The resulting images display the same phenomenology as the experimental results, showing deformation concentrated along micro-bands, probably similar to those reported in other studies [Gimbert et al., 2013; Kuhn, 1999]. The micro-bands observed in the DEM simulations are transient, as was reported in other numerical works [Maloney and Lemaître, 2006] where they were qualified of self-healing micro-cracks and distinguished from the final persistent shear-band.

If the nature of the transient micro-bands is understood, the picture of the formation of the final rupture is still incomplete. The permanent shear bands observed at the end of the loading do not correspond to a coalescence of the micro-bands until the size of the system is reached, nor to the growth of a particular micro-band, for example locked on a defect. Nevertheless, the formation of the final rupture plane is neither decorrelated of this process as we can see in Figure 2.22. There is a hierarchical imbrication of the two processes which still need to be unravelled. We will come back to those questions in the last section about my projects for the next few years.

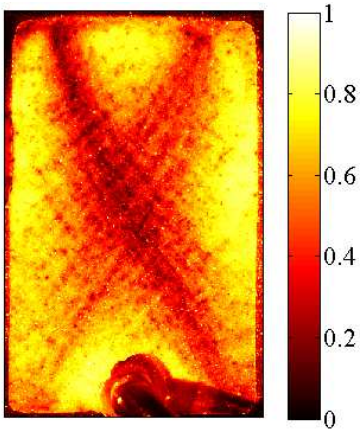

Figure 2.22: Correlation map near the rupture showing the hierarchical interaction between the fine structure due to the transient micro-bands and the premise of the future rupture planes.

We analyzed in this part the plastic flow observed during the quasi-static loading of a granular material. But in certain conditions, we have also observed during the loading micro-ruptures which behavior is closer to the phenomenology of the failure than of the micro-bands as they correspond to large collective rearrangements. I present the study of such micro-ruptures in the next section.

2.2.2 Micro-ruptures

Main associated publication: A. Amon, R. Bertoni, and J. Crassous, ***Phys. Rev. E* 87**, 012204 **(2013)**.

During the quasi-elastic loading of a granular material, several micro-ruptures can be observed before the global rupture of the material, forming stress drops along the loading curve (see Fig. 2.23 for an example of such drops in the ESPCI shear cell). Such micro-drops have been observed in different loading configurations [Nguyen et al., 2011; Le Bouil et al., 2014b] and are reminiscent of analogous behavior observed in metallic glasses [Klaumünzer et al., 2011] and to the precursors observed in studies of the onset of frictional sliding [Rubinstein et al., 2007]. A well-known granular material set-up where such regular micro-ruptures are observed is the progressively inclined box filled with sand [Nerone et al., 2003; Kiesgen de Richter, 2009; Duranteau, 2013]. In this system, the micro-ruptures occuring before the avalanche have been called precursors of the avalanche and have been shown to occur at regular angle increments until the destabilization of the pile. To our knowledge, in the case of the pre-avalanche behavior, no explanation of the regularity exists in the litterature, nor any numerical observation of the phenomenon [Staron et al., 2002, 2006; Welker and McNamara, 2011].

In the case of a sheared granular material in a scissometer (see subsection 2.2.1), our colleagues from ESPCI [Nguyen et al., 2011] have shown that micro-ruptures are observed during strain-rate imposed experiments along the otherwise quasi-elastic loading of the material (see Fig. 2.23(a)). The first micro-rupture is observed for a stress σ_r which is roughly the quarter of the stress σ_M at which the final rupture occurs, independently of the packing fraction of the preparation. In their

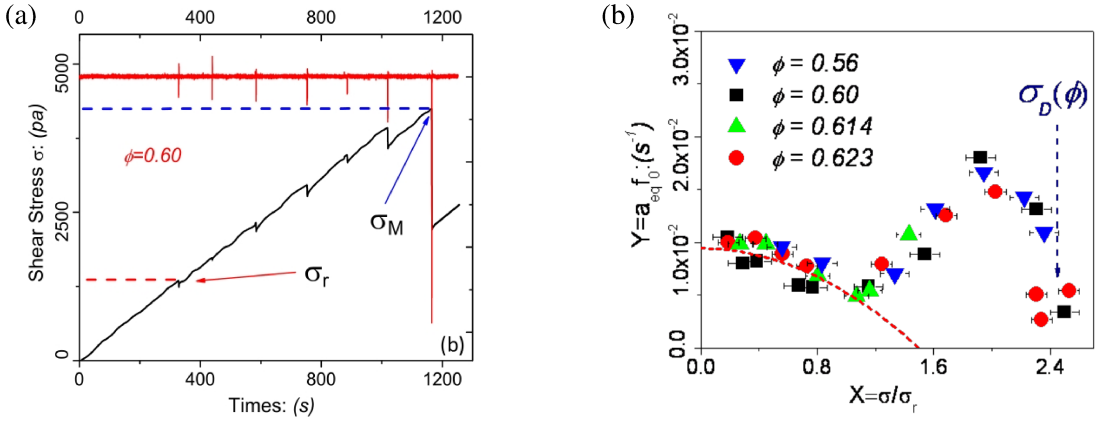

Figure 2.23: From [Nguyen et al., 2011]. (a) Loading curve of a granular material submitted to a shear ramp in a scissometer. Black line: shear stress σ as a function of time. Red line: derivative of the shear stress. σ_r is the first rupture observed along the loading curve, σ_M is the stress at which the failure occurs. (b) Rescaled effective ageing parameter characterizing the creep process in stress imposed experiments as a function of the imposed stress rescaled by σ_r. The red dashed line correspond to an interpretation in the framework of a SGR model; ϕ is the packing fraction.

interpretation of the behavior of the system in the framework of a SGR model, they have shown that this threshold σ_r corresponds to a minimum of the parameter characterizing the ageing of

the fluidity ((see Fig. 2.23(b)). The authors interpret this slowing down of the creep dynamics to large scale reorganization in the granular pile.

The input of our method of observation for the interpretation of the behavior of the shear material in the vicinity of a micro-rupture has been rather qualitative. We have evidenced an accumulation of spots just before stress drops and have shown that the stress drops correspond to micro-ruptures in the sample (see Fig. 2.17) [Amon et al., 2012]). A further study of the position of the rupture planes and the quantitative analysis of the spatio-temporal dynamics of the spots before the rupture was impeded by the smallness of the region of interest, although we had some clues that the radius of the rupture area increses with shear stress, as can be seen on Figure 2.24.

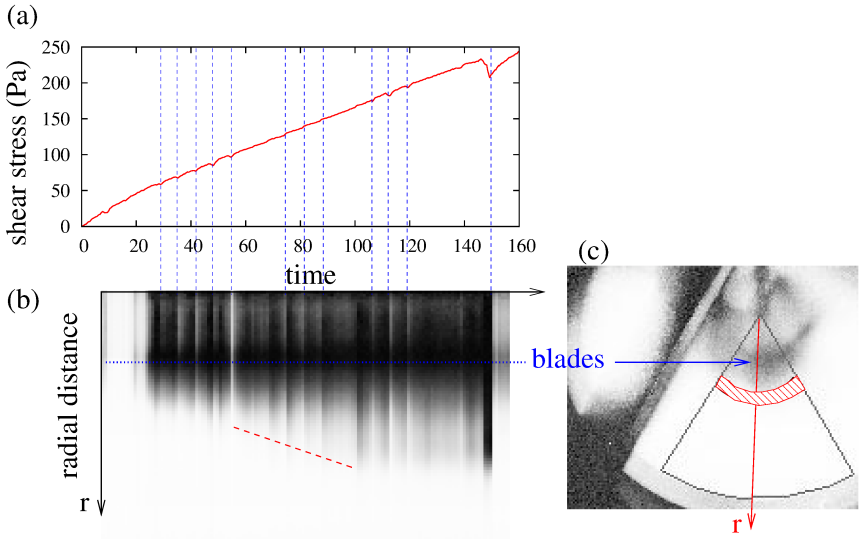

Figure 2.24: (a) Loading curves of a granular material submitted to a shear ramp in the scissometer of subsection 2.2.1: stress ramp as a function of time. (b) Spatio-temporal response of the granular: the average value of the correlation at a radial distance r from the middle of the cell is represented in grey levels as a function of r and time. (c) Correlation map of the surface of the scissometer. The region of interest is delimited by a black line. The values of the correlation are averaged over angle arcs at a given r. The position of the four-blades vane can be seen as well as the arm used for the angle measurements.

A better understanding of the micro-ruptures formation phenomenon has been achieved through the study of a progressively inclined granular pile. As said before, this configuration is rather standard in granular matter for the study of pre-avalanche phenomenology. The main previous experimental studies are of two types: direct imaging of the top free surface of the sample [Nerone et al., 2003; Kiesgen de Richter et al., 2012] and acoustic measurements [Zaitsev et al., 2008; Gibiat et al., 2009]. Those studies have shown the existence of two kind of movements in the sample: small rearrangements, implying only a few number of grains and large amplitude periodic events which have been called precursors. In order to give a new insights on this phenomenon, we designed an experimental setup allowing a visualization of the behavior of the grains in the depth of the sample by imaging the side of a box containing the granular material 2.25. Our observations evidenced that localized rearrangements, of the same type of those discussed in the previous sec-

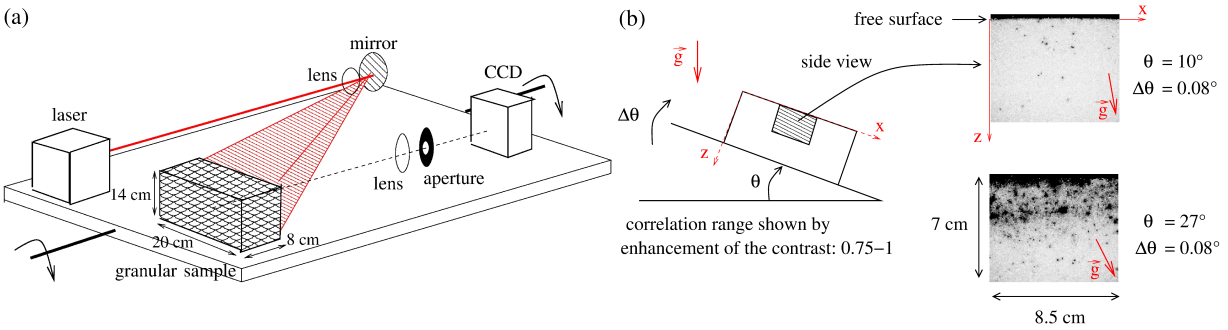

Figure 2.25: (a) Schematic of the experiment: the lightening and imaging setup as well as the granular sample are fixed on an rotating optical board. (b) The correlation maps correspond to a visualization of the deformation on the side of the sample. The angle increment between the images used for the correlation calculation is 0.08°.

tion and implying typically ten grains, are present from the very beginning of the tilting process and occur at all depths in the sample (see Fig. 2.25(b) at 10°). The density of rearrangements can be measured at a given depth under the surface as a function of the tilt angle θ (see Fig. 2.26(a)). At a given depth, the density of the spots increases with the shear, while at a given angle the density of the rearrangements decreases with the depth.

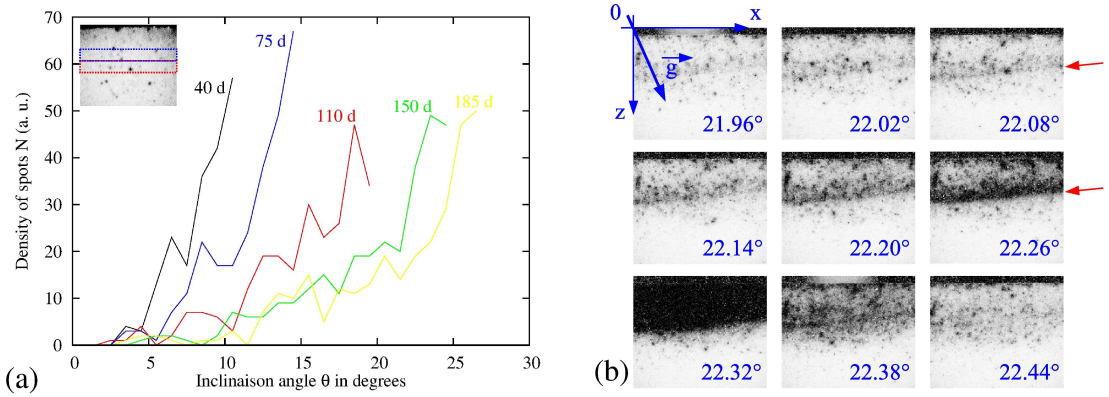

Figure 2.26: (a) Density of spots during the tilting process for different depths indicated in number of beads diameter under the free surface. (b) Successive correlation maps showing the formation of a micro-rupture.

We have also observed large events implying typically a layer of material parallel to the surface. Such micro-rupture can be seen in Figure 2.26(b) at 22.32°. The micro-rupture phenomenenology is mainly a function of the depth z under the free surface so that a spatio-temporal representation obtained by averaging the values of the correlation at each depth z allows a good visualization of the behavior of the sample during the quasi-static tilting of the pile (see Fig. 2.27(b)). We observe regularly spaced large events. The depth of those events increases linearly with the angle of inclination until the avalanche (see Fig. 2.27(a)). Those events occur from an angle θ_r typically around 15°, independently from the type of material, revealing an internal threshold well below the avalanche angle. It is striking to observe that while the slope of this linear behavior is material

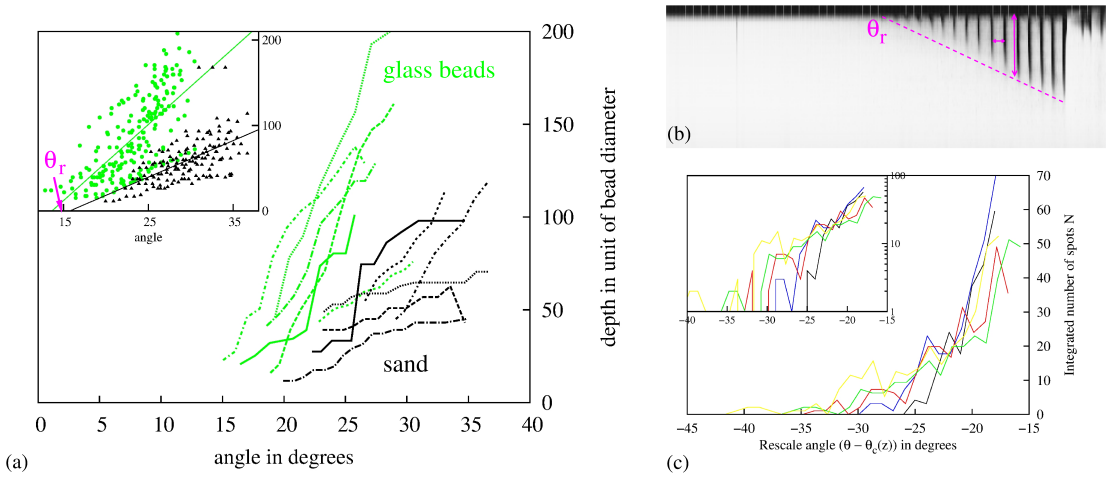

Figure 2.27: (a) Depth of the micro-ruptures as a function of the tilt angle for several experiments done with sand (black lines) and glass beads (green line). Inset: gathering of numerous experiments with linear fits. (b) Spatio-temporal diagram obtained from the correlation maps by averaging the correlation at constant depth z. (c) Density of spots as a function of the angle distance from the rupture.

dependent, the threshold is roughly the same for sand and glass beads. This linear relationship allows to shift the curves corresponding to the densities of rearrangements at different depths on a unique master curve (see Fig. 2.27(c)), showing that the critical number of spots before a micro-failure is the same independently of the depth. As that density decreases with depth, the angle at which a micro-rupture occurs increases with depth.

This phenomenology is coherent with the observations and analysis coming from the ESPCI setup, but also with our recent observations from the biaxial test [Le Bouil et al., 2014b]. Indeed, in the previous subsection (2.2.1.b) we have roughly described the deformation observed during a biaxial test as constituted of three phases: at first isolated rearrangements dominate, then (at about half the loading curve) intermitttent micro-bands appear and finally permanent shear-bands are observed after the rupture (see Fig. 2.19(a) in subsection 2.2.1.b). We can then understand the internal threshold (σ_r or θ_r) as the stress above which the coupling between the rearrangements can not be neglected. It is then logical that under this threshold a description using a "local" fluidity model which does not take into account the coupling is accurate but that it fails to describe the internal dynamics above σ_r when the coupling has to be taken into account (see Fig. 2.23(b) and [Nguyen et al., 2011]). In the continuity of our analysis of the coupling between the local rearrangements, we await this threshold to be determined by the elastic properties of the material, which should not depend a lot of the surface properties of the grains, explaining that we found a similar angle θ_r for the sand and the glass beads. On the contrary, the deformation induced by the micro-ruptures shear a few layers of grains on a characteristic depth which depends of the material [Komatsu et al., 2001], explaining the dependence of the depth of the micro-ruptures on the nature of the material [Amon et al., 2013].

Finally, what is really surprising is that a model developped to describe *fluids*, *i.e.* systems for which the temperature or a source of noise is an essential hypothesis, works so well for the

description of a granular system so far from its flowing state in experiments well isolated from mechanical noise sources. The study of the influence of noise in this context is a work-in-progress as will be seen in the last section.

2.2.3 Towards elasticity

I will now discuss two experiments where the issue of the elastic limit of the granular material is adressed. In the first experiment, we study the response of a granular pile to a homogeneous deformation obtained by thermal expansion. The second experiment concern an heterogeneous field of deformation: the response of a granular pile to a localized force.

2.2.3.a Homogeneous deformation: thermal expansion

Main associated publication: J. Crassous, M. Erpelding, and A. Amon, ***Phys. Rev. Lett.*** **103**, 013903 **(2009)**.

The study I present now is based on a method of measurement slightly different from the one used in the works discussed hitherto. Here, we do not seek for any spatial resolution but we take into account a parameter which can be changed in our interferometric technics but which is usually considered as a constant: the wavelength of the coherent light used to probe the sample. This experiment has been discussed previously in subsection 1.3.1 from the point of view of waves propagation in scattering materials. In the present part, I discuss how we can use this method to measure non-isotropic deformation in a granular material.

We have shown, in the case of multiple scattering, that an isotropic deformation can be compensated optically by tuning the wavelength. The experimental measurement is recalled in Figure 2.28(a): by modulating the wavelength of the coherent source during a thermal ramp, a correlation close to 1 can be recovered when the change of the wavelength compensates the isotropic deformation of the material. What was not specified when the scattering aspects of the

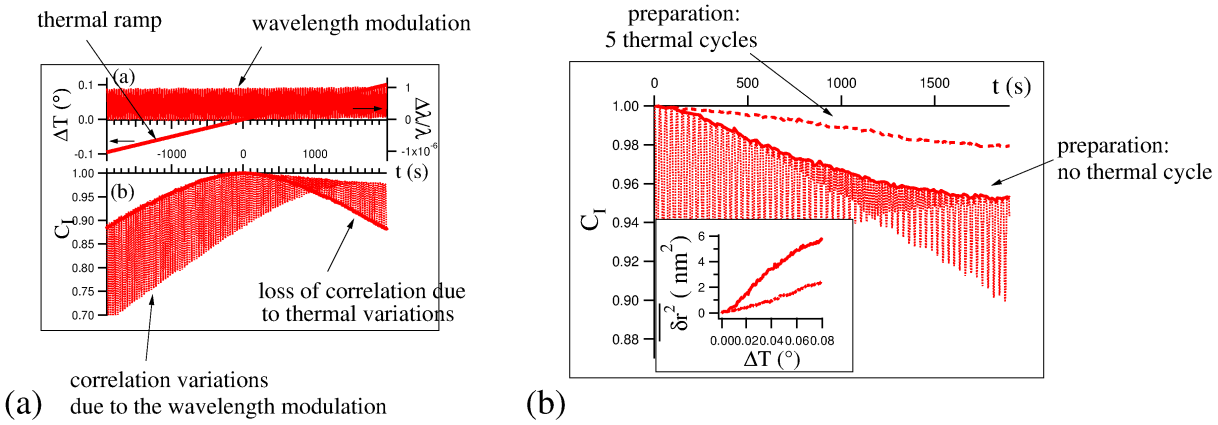

Figure 2.28: (a) (a) Top: temperature variation and modulation of the wavelength of the laser. Bottom: correlation obtained using $t = 0$ s as reference. Thick line: temperature variation alone; Fine line: combination of temperature variation and wavelength modulation. (b) Correlation recovered during expansion for two different preparations of the granular sample. Inset: non-isotropic part of the deformation obtained from the unrecoverable loss of correlation.

experiment has been discussed in subsection 1.3.1 is that those experimental results were obtained after a preparation of the granular material of several thermal cycles. When the material is not prepared in that way, less correlation is recovered (see Fig. 2.28(b)). At the maximum of recovered correlation the volumic deformation is always fully compensated, consequently the remaining part of the correlation loss can be directly connected to the non-isotropic part of the displacement. By considering that this nonisotropic part of the deformation originate from uncorrelated displacements, we obtain a measurement of the quadratic mean non-isotropic deformation (Insert of Fig. 2.28(b)). The result is in agreement with measurements reported in the literature of granular compaction provoked by temperature variation [Divoux, 2010].

This work needs to be pursued to obtain an extensive study of the non-isotropic part of the deformation with several underlying questions, such as the issue of the reversibility of that non-homothetic deformation when the thermal ramp is reversed: is there a part of the deformation which is not compensable, and consequently not isotropic, but which is fully reversible, and consequently elastic ? Such experiment is a part of the project I expose in the last section of this chapter.

2.2.3.b Heterogeneous deformation: response to a localized force

Main associated publication: M. Erpelding, A. Amon, and J. Crassous, ***Europhys. Lett.*** **91**, 18002 **(2010)**.

The question of the elastic limit of a non-cohesive granular material and of the response of this material when submitted to cycles of force of very small amplitude is in fact one of the first question we adressed with our spatially-resolved method of measurement of small deformation. During the PhD thesis of Marion Erpelding, we have studied the mechanical response of a granular pile to a localized force and we have characterized experimentally the main differences between the response of a granular sample and of an elastic reference media. The experimental setup is shown on Figure 2.29(a) and (b): it is our typical setup to obtain spatially resolved map of deformations. We used a vibrator to exert the localized force on the material but the frequency used for the force ramps was very small in order to stay in a quasi-static limit.

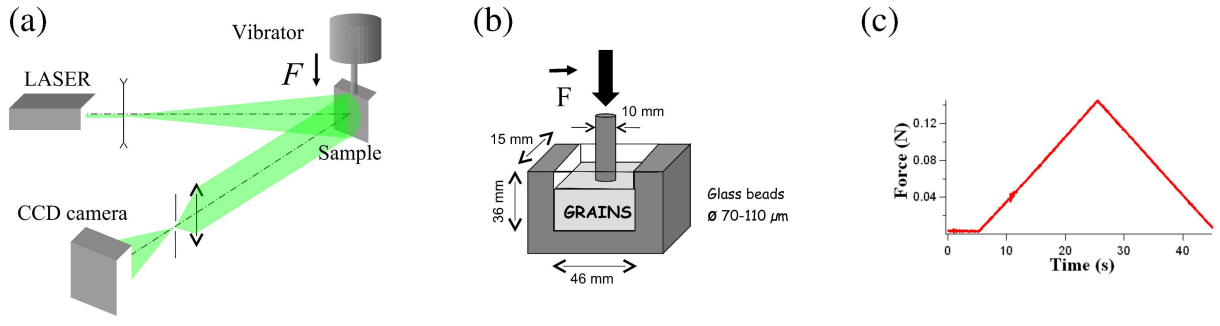

Figure 2.29: (a) Schematic of the setup. (b) Details of the granular sample. (c) Typical force ramp, note the small ampitude of the maximal force and the large value of the period of the cycle.

First, we have studied the spatial repartition of the deformation of a granular material submitted to a localized force. Figure 2.30(a) shows the observed spatial repartition of the deformation using always the initial speckle image from the unloaded sample as a reference for the calculation of correlation in order to observe the response of the system to a varying force increment and its reversibility. We do not observe any large heterogeneities or a directivity in the deformation as was proposed in some models [Bouchaud et al., 1995]. The response qualitatively resembles to an elastic response with a smooth, bulbous form.

We have studied the response of the system as a function of the number of cycles. The first cycle is characterized by a large amount of irreversibility (see Fig. 2.30(b)) while from the fourth cycle, the curve is almost closed: the response can be considered as reversible (see Fig. 2.30(c)) and studied as an elastic response.

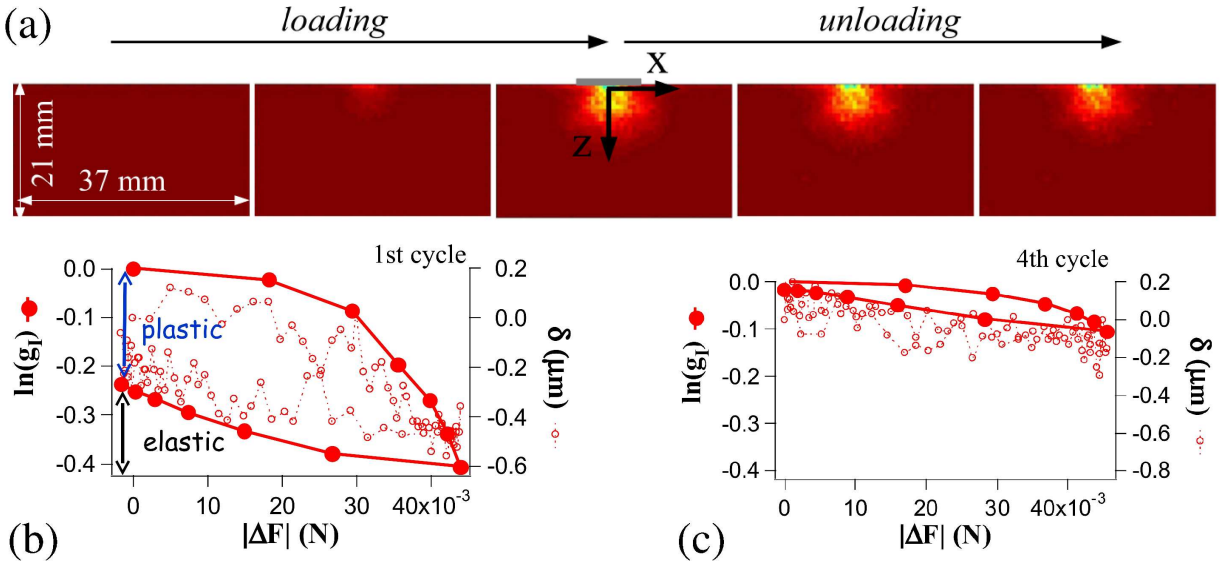

Figure 2.30: (a) Correlation maps for the first force cycle using the begining of the cycle as image reference. (b) and (c) thick line and filled circles: logarithm of the correlation for one pixel of the map as a function of the force increment; dotted line and open circles: displacement of the tip exerting the localized force. (b) first cycle, (c) fourth cycle.

As we are in a case of an heterogeneous apply stress, the question of the separation of the spatial dependency from the force increment dependency may be adressed. We have found that for two different force increments, $\epsilon(\Delta F_1, \mathbf{r})/\epsilon(\Delta F_2, \mathbf{r})$ does not depend of the position $\mathbf{r}$, which means that we can indeed write:

$$\epsilon(\Delta F, \mathbf{r}) = \psi(\Delta F)\zeta(\mathbf{r}), \tag{2.4}$$

where we determine $\psi(\Delta F)$ by considering that $\epsilon(\Delta F_{max}, \mathbf{r}) = \zeta(\mathbf{r})$. The curve in Figure 2.31(a) shows $\epsilon(\Delta F, \mathbf{r})/\psi(\Delta F)$ from all the points of maps corresponding to five different values of the force increment ΔF collapse on the line of slope 1, confirming this decomposition.

The spatial depedence is not $\propto 1/r$ as awaited for the Boussinesq solution for an elastic sample. This observation is not so surprising as even for an elastic material the friction on the glass wall would create a screening of the force because of the friction [Ovarlez and Clément, 2005]. The

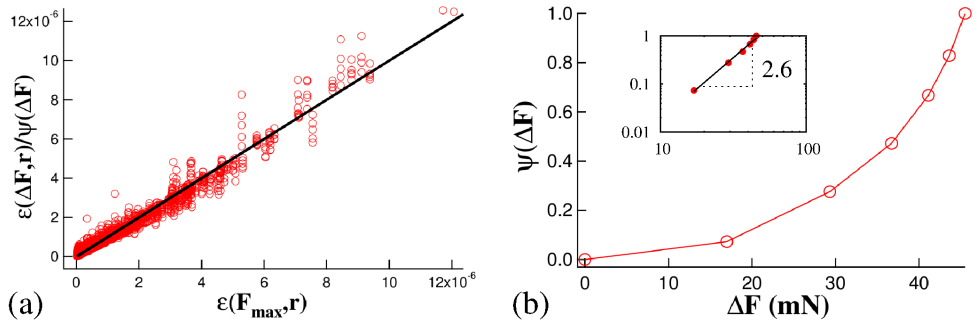

Figure 2.31: (a) Validation of the decomposition of Eq. 2.4 using all the values of the metapixels of maps corresponding to five force increments. (b) Dependency on the force increment in Eq. 2.4 as a function of the force increment ΔF.

dependence of $\psi(\Delta F)$ with the force increment ΔF is shown in Figure 2.31(b). We have no interpretation of this nonlinear dependence, which is incompatible with a nonlinear dependence which would be caused by the Hertz law.

In fact, when studying the response of the system to a large number of cycles as shown on Figure 2.32(a), we observe that apart from the first one, the following cycles are indeed almost closed, but we can notice that the maximum of the deformation reached for the same force increment decreases with the number of cycle: the stiffness increases with the number of cycles. It suggests a slow compaction of the material. Moreover, when the cycles are rescaled (see

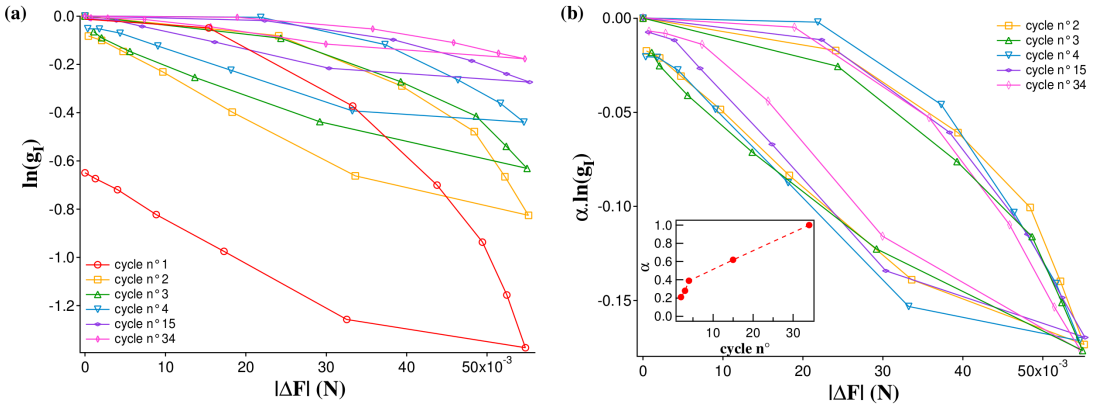

Figure 2.32: From [Erpelding, 2010]. (a) Logarithm of the correlation measured for one pixel of the correlation map as a function of the force increment for different number of force cycles. (b) Rescaling of the closed cycles. Inset: scaling factor as a function of the cycle number.

Fig 2.32(b)), even if the reversibility is good, the cycles are open. The presence of that area could originate from some dissipative process large enough to result in an open cycle but which does not lead to irreversible plastic deformation measurable by our method. But the curvature of the cycle could also perhaps be linked to some optical effect we have neglected so far.

This work let consequently open several questions and it is the reason why I ended the presentation of our works on granular material with this study although it was historically one of our first

work on granular material using the spatially-resolved method of measurement of the deformation.

In conclusion, the scenario coming from soft glassy theories describing the plasticity in amorphous materials as coming from local plastic events interacting through elasticity is in agreement with our experimental observation in granular materials. Nevertheless, a lot of questions are still open. First, this coupling between the local events need to be further studied, in order to understand the conditions of apparition of cooperative effects in the material. Moreover, we have seen that the formation of the final shear-band as well as the phenomenology of micro-ruptures preceding it are still unclear. To finish with, the characterization of the response of a granular material to a cyclic load in the reversible limit is still largely to be understood.

2.3 Work-in-progress and projects

I will now describe my research projects for the next few years which concern mainly questions linked to the plasticity of granular materials. Following the conclusion of the previous part, my projects aim at moving from very small deformation and the study of the elastic limit to large deformation with well-established shear-bands.

I present the different steps of that project in the following parts: first, I discuss the experiment we have begun to develop in order to study the response of granular materials submitted to small thermal cycles. Secondly, we will persue our work of characterization of the local rearrangements. Finally we have begun to work on sheared granular materials where shear bands are well established and study the mechanical noise generated outside the shear band [Nichol et al., 2010; Reddy et al., 2011].

2.3.1 Elastic limit, cycles and contact plasticity

The first part of my project is devoted to the study of the response of a granular sample submitted to thermal cycles in the small deformation limit. The goal is to combine the method of compensation of volumic deformation by tuning of the wavelength to the spatial resolution which can be acheived in backscattering. Our previous experiment of thermal expansion [Crassous et al., 2009] was also limited by the small range of tunability of the laser. Indeed, lasers emitting in the visible range are not widely tunable without mode hop contrary to infrared source. In collaboration with Julien Fade from the "Optics and Photonics" group at IPR, we have acquired an infrared camera and built a bench for DWS using a widely tunable infrared laser. The first measurements we have done confirm the feasibility of the method in the near infrared range to obtain spatially-resolved maps of deformation. The goal is then to explore the limit of a large number of thermal expansion cycles, using noise-reduction schemes to acheive measurements of very small decorrelation [Skipetrov et al., 2010].

Granular materials display small rearrangements when submitted to small temperature variations [Divoux, 2010] and we await contact plasticity even for very small thermal cycles. A study of the influence of cohesive forces will be done to understand if the limit of dry granular materials has remarkable characteristics, especially concerning the residual plasticity observed during cyclic

forcing of very small amplitude and the fragility of the pile. Our set-up should allow us to explore experimentally the reversible non-isotropic part of the deformation. As discussed in the state of the art, specific features of this response is awaited for disordered materials because of the non-affine displacement and we intend to measure that part of the deformation in our system.

2.3.2 Coupling of local rearrangements and shear-band formation

The second part of the project will be dedicated to the pursuit of the characterization of local, isolated plastic events depending on the preparation of the sample. In particular, the influence of parameters as cohesion or volumic fraction will be analyzed as well as the conditions of apparition of coherent structures. This part of the project will be done in close collaboration with Sean McNamara from the "Discrete Media Group". The parallel study of DEM simulation and of experiments in similar systems has indeed proven to be very inspiring for the understanding of our observations in recent works [Le Bouil et al., 2014a].

We also continue our collaboration with Eric Clément from PMMH and the study of local rearrangements in sheared granular materials. Our main interests are for the spatio-temporal dynamics of the appearance of the spots and the influence of noise on the fluidity [Espíndola et al., 2012]. A post-doctoral fellow, Adeline Pons (PMMH, ESPCI, Paris), is presently working on this project.

Those works linked to the triggering and coupling of local rearrangements from an experimental and numerical point of view should lead to a better understanding of the process of the building-up of the plastic flow during the deformation of a granular pile and of the final shear-bands formation. The analysis of the hierarchical structure we observed at the transition between the structuration of the plastic flow and the rupture, as has been shown in Figure 2.22 is a work-in-progress. Notably, this work has led us to work on methods of characterization of the spatial structuration, such as multiscale analysis [Gimbert et al., 2013]. In this context, we have contributed to a study concerning image analysis tools for the characterization of textures in images [Lehoucq et al.] and we are collaborating with Jérôme Weiss (LGGE UMR 5183, UJF, Grenoble) and David Amitrano (ISTerre UMR 5275, UJF, Grenoble) on this side of the project, and more generally on the problem of rupture [Gimbert et al., 2013].

2.3.3 "Mechanical noise" and fluidity

The last part of the project is dedicated to the understanding of the behavior of the system when it is flowing. When a granular system is submitted to a large enough shear rate, the flow localized in a shear band while the rest of the system displays much smaller, creep-type, displacements [Komatsu et al., 2001; Chambon et al., 2003]. Because of the shear band, the rest of the system is fluidized by a "mechanical noise" [Nichol et al., 2010; Reddy et al., 2011], and nonlocal fluidity models integrating this noise have been proposed [Kamrin and Koval, 2012].

We have done experiments with Olivier Pouliquen and Yoël Forterre from IUSTI in Marseille who have built a Couette cell for a granular material [Reddy et al., 2011]. In such a rheometer, at constant shear rate, a shear band with a spatial extension of tens of grain diameters forms near the rotor. It leads to a spatial separation of a granular flow and a granular creeping solid in the same rheometer. We have begun to study the part of the system outside the shear band with our

measurement method. Our first observations are very promising.

To conclude this part, I have presented here what I considered as the most important part of my work of the past few years. I think those experimental studies have allowed a great improvement in the understanding of the plasticity of granular materials. I have replaced those findings in the present context of research in the field of soft glassy materials to underline the generality of those results.

To summerize those works, we have shown experimentally that plasticity in sheared granular materials occur in the form of local plastic events which coupled through elasticity. This coupling lead to the structuration of the plastic flow with the formation of transient micro-bands of growing size during the loading. This coupling is also connected to the occurence of micro-ruptures in the material, the condition of formation of which are still unclear. The transient structuration of the flow progressively couple to a larger-scale mechanism which lead to the formation of the final shear-band in a process still not understood. Finally, our works have risen several new and exciting issues while answering to old questions.

Chapter 3

Nonlinear dynamics

In this chapter, I will briefly described my other research interests, all connected to nonlinear dynamics. Indeed, from the beginning of my PhD thesis in 2000 until 2007, my research activities were dedicated to nonlinear optics. I studied the temporal dynamics of several nonlinear optical systems, mainly optical parametric oscillators. Those works were experimental, numerical and theoretical. I am still having a research activity connected to nonlinear dynamics through collaborations with experimentalists from several fields. My work in this domain is now solely theoretical and numerical and concern the modeling of two very different systems. The first collaboration is internal to the Soft Matter Group. It is a project initiated by Pascal Panizza in collaboration with Laurent Courbin, for the study of traffic of droplets in microfluidics networks. The second collaboration is with Denis Michel from the Biology Departement of Université Rennes 1 ("Interactions Cellulaires et Moléculaires", UMR 6026) and is connected to genetic regulation.

In the following I will not present my works concerning nonlinear optics[1], because most of those studies are directly linked to my PhD thesis. I will rather expose my recent collaborations. Nevertheless, I would like to underline here the continuity in this branch of my researchs. As an example, I will mention my collaboration with Thomas Erneux ("Optique Nonlinéaire Théorique" group, ULB, Bruxelles), in the group of whom I spent a month the first year of my PhD and who I invited in Rennes few years ago to give lectures about delay equations and discuss of such delay models for microfluidic networks. The universality of the mathematical tools explain the possibility to have a theoretical contribution in widely different fields.

The outline of the chapter is the following: the first section concerns traffic in microfluidics devices and the second section genetics.

[1]Publications concerned: [Amon et al., 2003; Amon and Lefranc, 2004; Brunel et al., 2005; Amon and Lefranc, 2007; Amon et al., 2009].

3.1 Traffic and microfluidics

Main associated publications:

- D. A. Sessoms, A. Amon, L. Courbin, and P. Panizza, "Complex dynamics of droplet traffic in a bifurcating microfluidic network: Periodicity, multistability, and selection rules", ***Phys. Rev. Lett.*** **105**, 154501 **(2010)**.
- A. Amon, A. Schmit, L. Salkin, L. Courbin, and P. Panizza, "Path selection rules for droplet trains in single-lane microfluidic networks", ***Phys. Rev. E*** **88**, 013012 **(2013)**.

Understanding the flow of discrete elements through networks is of importance for numerous phenomena, as for example diphasic flows in porous media, cells in blood flows [Carr and Lacoin, 2000], microfluidic devices [Stone et al., 2004; Joanicot and Ajdari, 2005] or even car traffic. Addressing this issue requires a description of the mechanisms that govern flow partitioning at a node. In the case of diluted flows of droplets in microfluidic networks, a droplet reaching a node will flow in the arm having the smaller hydrodynamic resistance [Engl et al., 2005]. Despite this robust and simple rule, a system as simple as a regular train of droplets reaching an asymmetric loop exhibits complex dynamics [Jousse et al., 2006; Fuerstman et al., 2007; Schindler and Ajdari, 2008; Sessoms et al., 2009; Cybulski and Garstecki, 2010]. Periodic and aperiodic behaviors have been observed with complex patterns of the repartition of the droplets (see Figure 3.1).

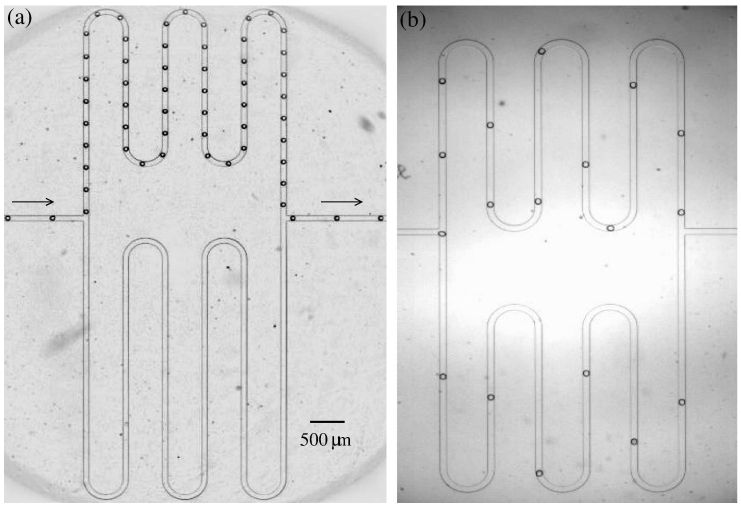

Figure 3.1: Examples of repartition of droplet trains in asymmetric loops. (a) Filter regime: all the droplets flow through the shortest arm. (b) Repartition regime: the droplets are choosing one or the other arm depending on the number of droplets already present in each arms of the loop. Complex patterns of repartition are then observed.

Such complexity emerges from time-delayed feedback: the presence of droplets in a channel increases its hydrodynamic resistance, so that the path selection of successive droplets at the node is affected by the trajectories of the previous droplets currently in the loop [Engl et al., 2005; Jousse et al., 2006]. We can then understand the behavior observed in Figure 3.1. When the train of droplets is very diluted, the hydrodynamic resistance of the shorter arm, even containing droplets, stays smaller than the hydrodynamic resistance of the long arm and the droplets suc-

cessively choose the short arm when reaching the node (*filter* regime, case of Fig.3.1(a)). When the distance between the droplets decreases, the hydrodynamic resistance of the short arm full of droplets will exceed the hydrodynamic resistance of the empty long arm and then each incoming droplet will choose one or the other arm depending on the paths followed by all the droplets still present in the system. The resulting pattern of repartition is complex (*repartition* regime, case of Fig.3.1(b)) [Engl, 2006].

From the point of view of nonlinear dynamics, this system is governed by delay equations, typical of systems with feedback loops. When nonlinear interactions are at play together with delays, complex dynamics can be observed [Erneux, 2009].

I have worked on the numerical and theoretical part of this project. We were able to propose for the first time a complete description of the response of this system allowing a full understanding of its dynamics [Sessoms et al., 2010a]. This description is based on a model leading to a discrete dynamics of a binary variable, and thus belongs to the class of cellular automata. We have shown that the dynamics is periodic and that it can be characterized by two quantities invariant for a set of parameters. We have predicted theoretically the bifurcations between different regimes and account for the values of the invariants in function of the relevant physical parameters of the system. The comparison between the theoretical predictions and numerical simulations are shown in Figure 3.2(a) and (b). The figures give this period T_{cyc} in function of the inter-droplets distance λ in fine line. Numerical simulations taking into account the fluctuations of the velocity in the system at each coming in and out of droplets also lead to periodic regims. The periods observed numerically are the black dots in Figure 3.2(a) and (b). The analytical model accurately accounts for the main trend of the behavior. The very long periods observed numerically correspond to set of parameters near the bifurcations between two well-defined plateau.

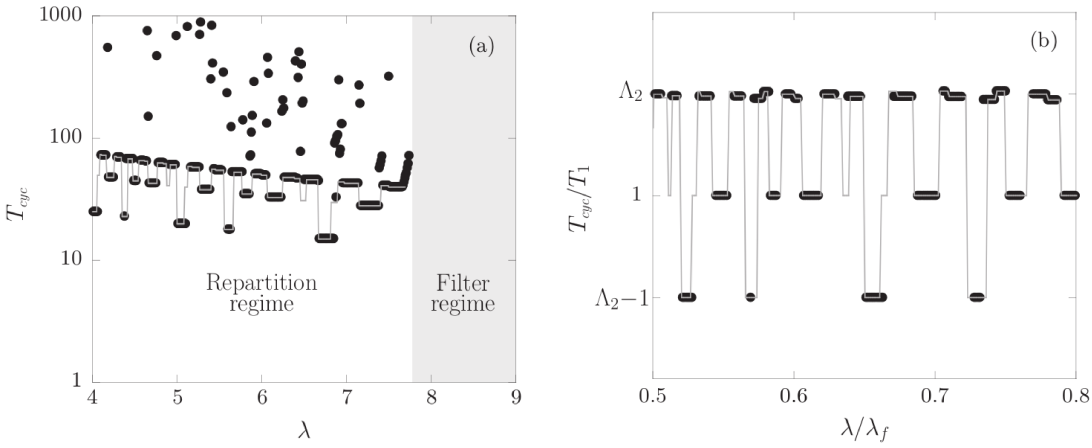

Figure 3.2: (a) Period of the pattern of repartition observed as a function of the distance λ between the droplets. The time is in unit of the inverse droplet rate at the node, the lengths have arbitrary units. The solid line is calculated using the discrete theoretical model. Filled circles stand for numerical results. (b) Enlargissement of the bifurcation diagram in rescaled unity: λ_f characterizes the transition between the filter regime and the repartition regime, T_1 is the time needed for a droplet to go through the short arm, Λ_2 is the ratio of the lengths of the two arms.

The experimental observations are well described by our predictions [Sessoms et al., 2010a]. In particular, we have observed experimentally a phenomenon called multistability between different

periodic regimes that we were able to reproduce numerically by taking into account noise in numerical simulation. We have also studied more complex networks [Amon et al., 2013], showing that the analytical results obtained for the asymetric loop can be generalized to more complex geometries. For particular classes of network topology, we have rationalized the existence of partial filter regimes for which only some branches of the network are explored while other paths are never taken. In contrary to the "simple" asymetric loop for which we were able to extract invariant quantitites characterizing the period and the spatial pattern of the regime, the dynamics of higher level networks is dependent of the initial conditions because of extra degrees of freedom, limiting the possibility of extension of the discrete model, while a continuous approach leads to the prediction of the fraction of droplets taking the different paths.

3.2 Gene regulation

Main associated publications:

- F. Nicol-Benoit, A. Amon, C. Vaillant, P. le Goff, Y. le Dréan, F. Pakdel, G. Flouriot, Y. Valotaire, and D. Michel, "A Dynamic Model of Transcriptional Imprinting Derived from Vitellogenesis Memory Effect", ***Biophys. J.*** **101**, 1557 **(2011)**.
- S. Lecomte, L. Reverdy, C. Le Quement, F. Le Masson, A. Amon, P. Le Goff, D. Michel, E. Christians and Y. Le Dréan, "Unravelling Complex Interplay Between Heat Shock Factor 1 And 2 Splicing Isoforms", ***PLoS One*** **8**, (2) e56085 **(2013)**.

Collaborations between physicists, in particular of the same field, is rather easy in the sense that we have the same language and we share common appraches facing a phenomenon to study and interpret it. Collaborations between scientists from very different fields is much more difficult. I have worked with Denis Michel, Professor in the Biology Departement of the University, and he has needed a lot of patience and perseverance to explain to me the basics of modeling in biology. My work on those projects was purely on the mathematical part and I will give here only the general framework of the problematic, which is link to epigenetic memory.

Information transmission in living systems does not rely only on the sole genetic material but also on epigenetic mechanisms governing the gene expression. The present understanding of those mechanisms of regulation relies on the existence of static markers specifying if the gene must be expressed or repressed. The possibility of dynamical mechanisms underlying this expression instead of static markers is rarely considered in experimental studies even though such interpretations are rather common in theoretical biology. In those models the current expression is understood as an equilibrium state of a complex dynamical system, *i.e.* an attractor for the gene expression in the complex networks of interaction of the machinery of gene regulation.

In this context, we have proposed a dynamical mechanism explaining a memory effect observed in vitellogenesis, in which the expression of a gene is modified by a past exposition to hormons. This model has been confronted to experimental measurements quantifying the variables of the considered dynamical system.

In this chapter, I have summarized some of my recent works connected to nonlinear dynamics. This field of research used to be my main specialty, hence my participation to the organizing committee of the summer school "Nonlinear Dynamics in Peyresq" and my M2 lectures "Nonlinear dynamics and chaos". My past works in this field has given me a good knowledge of the mathematical tools that have been developped in this research field and which are not so widespread. I have still many interests in this field, which allow enriching transversal collaborations as the ones described in this chapter.

General conclusion

In this dissertation, I gave a general overview of my scientific career and I presented the main research works I have undertaken since my nomination as an Assistant Professor at the Université de Rennes 1 in 2004.

I gave a synthetic description of the results and highlights of my research activities in the respective fields of light scattering, granular materials and nonlinear dynamics. I replaced all those works in the context of the research advances in each of those fields and I gave the main progresses that our studies have allowed. I more particularly detailed my works linked to the plasticity of granular materials. This field has became by now my principal subject of research and I gave a description of my projects for the next few years in this domain. Those projects still concern the plasticity of granular media and the localization of the deformation in heterogeneous materials as those issues are still challenges for the understanding of the unjamming transition and the failure process in granular materials.

Bibliography

A. Amon and M. Lefranc. Topological signature of deterministic chaos in short nonstationary signals from an optical parametric oscillator. *Physical Review Letters*, 92(9):094101, 2004.

A. Amon and M. Lefranc. Mode hopping strongly affects observability of dynamical instability in optical parametric oscillators. *The European Physical Journal D*, 44(3):547–556, 2007.

A. Amon, M. Nizette, M. Lefranc, and T. Erneux. Bursting oscillations in optical parametric oscillators. *Physical Review A*, 68(2):023801, 2003.

A. Amon, P. Suret, S. Bielawski, D. Derozier, and M. Lefranc. Cooperative oscillation of nondegenerate transverse modes in an optical system: Multimode operation in parametric oscillators. *Physical Review Letters*, 102:183901, 2009.

A. Amon, V. B. Nguyen, A. Bruand, J. Crassous, and E. Clément. Hot spots in an athermal system. *Physical Review Letters*, 108(13):135502, 2012.

A. Amon, A. Schmit, L. Salkin, L. Courbin, and P. Panizza. Path selection rules for droplet trains in single-lane microfluidic networks. *Physical Review E*, 88(1):013012, 2013.

B. Andreotti, Y. Forterre, and O. Pouliquen. *Les milieux granulaires: entre fluide et solide*. EDP sciences, 2012.

A. S. Argon. Plastic deformation in metallic glasses. *Acta Metallurgica*, 27(1):47 – 58, 1979.

A. P. F. Atman, P. Brunet, J. Geng, G. Reydellet, G. Combe, P. Claudin, R. P. Behringer, and E. Clément. Sensitivity of the stress response function to packing preparation. *Journal of Physics: Condensed Matter*, 17(24):S2391, 2005.

C. Baravian, F. Caton, J. Dillet, and J. Mougel. Steady light transport under flow: characterization of evolving dense random media. *Physical Review E*, 71(6):066603, 2005.

J.-L. Barrat. Microscopic elasticity of complex systems. In *Computer Simulations in Condensed Matter Systems: From Materials to Chemical Biology Volume 2*, pages 287–307. Springer, 2006.

B. J. Berne and R. Pecora. *Dynamic Light Scattering With Applications to Chemistery, Biology, and Physics*. Dover Publication Inc., 2000.

L. Berthier and G. Biroli. A statistical mechanics perspective on glasses and aging. *Encyclopedia of Complexity and Systems Science*, 2009.

P. Bésuelle and J. W. Rudnicki. Localization: Shear bands and compaction bands. In Y. Guéguen and M. Boutéca, editors, *Mechanics of Fluid-Saturated Rocks*, volume 89, pages 219–321. Academic Press, New York, 2004.

D. Bicout and G. Maret. Multiple light scattering in taylor-couette flow. *Physica A: Statistical Mechanics and its Applications*, 210(1):87–112, 1994.

D. Bicout and R. Maynard. Diffusing wave spectroscopy in inhomogeneous flows. *Physica A: Statistical Mechanics and its Applications*, 199(3):387–411, 1993.

D. Bicout, E. Akkermans, and R. Maynard. Dynamical correlations for multiple light scattering in laminar flow. *Journal de Physique I*, 1(4):471–491, 1991.

L. Bocquet, A. Colin, and A. Ajdari. Kinetic theory of plastic flow in soft glassy materials. *Physical Review Letters*, 103(3):036001, 2009.

L. Bonneau, B. Andreotti, and E. Clément. Evidence of rayleigh-hertz surface waves and shear stiffness anomaly in granular media. *Physical Review Letters*, 101:118001, 2008.

J.-P. Bouchaud, M. E. Cates, and P. Claudin. Stress distribution in granular media and nonlinear wave equation. *Journal de Physique I*, 5(6):639–656, 1995.

J.-P. Bouchaud, P. Claudin, D. Levine, and M. Otto. Force chain splitting in granular materials: A mechanism for large-scale pseudo-elastic behaviour. *The European Physical Journal E*, 4(4): 451–457, 2001.

E. Bouchbinder, J. S. Langer, and I. Procaccia. Athermal shear-transformation-zone theory of amorphous plastic deformation. i. basic principles. *Physical Review E*, 75(3):036107, 2007.

M. Brunel, A. Amon, and M. Vallet. Dual-polarization microchip laser at 1.53 μm. *Optics letters*, 30(18):2418–2420, 2005.

R. T. Carr and M. Lacoin. Nonlinear dynamics of microvascular blood flow. *Annals of biomedical engineering*, 28(6):641–652, 2000.

M. E. Cates, J. P. Wittmer, J.-P. Bouchaud, and P. Claudin. Jamming, force chains, and fragile matter. *Physical Review Letters*, 81:1841–1844, 1998.

G. Chambon, J. Schmittbuhl, A. Corfdir, J.-P. Vilotte, and S. Roux. Shear with comminution of a granular material: Microscopic deformations outside the shear band. *Physical Review E*, 68 (1):011304, 2003.

K. Chen, M. L. Manning, P. J. Yunker, W. G. Ellenbroek, Z. Zhang, A. J. Liu, and A. G. Yodh. Measurement of correlations between low-frequency vibrational modes and particle rearrangements in quasi-two-dimensional colloidal glasses. *Physical Review Letters*, 107(10):108301, 2011.

L. Cipelletti and E. R. Weeks. *Dynamical Heterogeneities in Glasses, Colloids and Granular Media*, chapter Glassy dynamics and dynamical heterogeneity in colloids, pages 110–151. Oxford University Press, 2011.

S. N. Coppersmith, C.-H. Liu, S. Majumdar, O. Narayan, and T. A. Witten. Model for force fluctuations in bead packs. *Physical Review E*, 53(5):4673, 1996.

J. Crassous. Diffusive wave spectroscopy of a random close packing of spheres. *The European Physical Journal E*, 23:145–152, 2007.

J. Crassous, J.-F. Metayer, P. Richard, and C. Laroche. Experimental study of a creeping granular flow at very low velocity. *Journal of Statistical Mechanics: Theory and Experiment*, 2008(03): P03009, 2008.

J. Crassous, M. Erpelding, and A. Amon. Diffusive waves in a dilating scattering medium. *Physical Review Letters*, 103(1):013903, 2009.

O. Cybulski and P. Garstecki. Dynamic memory in a microfluidic system of droplets traveling through a simple network of microchannels. *Lab on a Chip*, 10(4):484–493, 2010.

J. C. Dainty, editor. *Laser Speckle and Related Phenomena*. Springer-Verlag, 1984.

O. Dauchot, G. Marty, and G. Biroli. Dynamical heterogeneity close to the jamming transition in a sheared granular material. *Physical Review Letters*, 95:265701, 2005.

C. Derec, A. Ajdari, and F. Lequeux. Rheology and aging: A simple approach. *The European Physical Journal E*, 4(3):355–361, 2001.

J. Desrues and R. Chambon. Shear band analysis and shear moduli calibration. *International Journal of Solids and Structures*, 39(13):3757–3776, 2002.

J. Desrues and I.-O. Georgopoulos. An investigation of diffuse failure modes in undrained triaxial tests on loose sand. *Soils and foundations*, 46(5):585–594, 2006.

J. Desrues and G. Viggiani. Strain localization in sand: an overview of the experimental results obtained in grenoble using stereophotogrammetry. *International Journal for Numerical and Analytical Methods in Geomechanics*, 28(4):279–321, 2004.

T. Divoux. *Bruit et fluctuations dans les écoulements de fluides complexes*. PhD thesis, Thèse de doctorat, Ecole Normale Supérieure de Lyon, 2009.

T. Divoux. Invited review: Effect of temperature on a granular pile. *Papers in Physics*, 2:020006, 2010.

T. Divoux, H. Gayvallet, and J.-C. Géminard. Creep motion of a granular pile induced by thermal cycling. *Physical Review Letters*, 101(14):148303, 2008.

L. Djaoui and J. Crassous. Probing creep motion in granular materials with light scattering. *Granular Matter*, 7:185–190, 2005.

M. Duranteau. *Dynamique granulaire à l'approche de l'état critique*. PhD thesis, Thèse de doctorat, Université de Rennes 1, 2013.

A. Duri and L. Cipelletti. Length scale dependence of dynamical heterogeneity in a colloidal fractal gel. *EPL (Europhysics Letters)*, 76(5):972, 2006.

A. Duri, D. A. Sessoms, V. Trappe, and L. Cipelletti. Resolving long-range spatial correlations in jammed colloidal systems using photon correlation imaging. *Physical Review Letters*, 102(8): 085702, 2009.

D. J. Durian, D. A. Weitz, and D. J. Pine. Multiple light-scattering probes of foam structure and dynamics. *Science*, 252(5006):686–688, 1991.

W. Engl. *Gestion de gouttes sur un réseau millifluidique: exemples d'analyse haut débit et de mise en forme de matériaux*. PhD thesis, Thèse de doctorat, Université de Bordeaux 1, 2006.

W. Engl, M. Roche, A. Colin, P. Panizza, and A. Ajdari. Droplet traffic at a simple junction at low capillary numbers. *Physical Review Letters*, 95(20):208304, 2005.

T. Erneux. *Applied Delay Differential Equations*, volume 3. Springer, 2009.

M. Erpelding. *Étude expérimentale de micro-déformations dans des matériaux hétérogènes par diffusion de la lumière*. PhD thesis, Thèse de doctorat, Université de Rennes 1, 2010.

M. Erpelding, A. Amon, and J. Crassous. Diffusive wave spectroscopy applied to the spatially resolved deformation of a solid. *Physical Review E*, 78(4):046104, 2008.

M. Erpelding, B. Dollet, A. Faisant, J. Crassous, and A. Amon. Diffusing-wave spectroscopy contribution to strain analysis. *Strain*, 49(2):167–174, 2013.

J. D. Eshelby. The determination of the elastic field of an ellipsoidal inclusion, and related problems. *Proceedings of the Royal Society of London. Series A. Mathematical and Physical Sciences*, 241(1226):376–396, 1957.

D. Espíndola, B. Galaz, and F. Melo. Ultrasound induces aging in granular materials. *Physical Review Letters*, 109(15):158301, 2012.

M. L. Falk and J. S. Langer. Dynamics of viscoplastic deformation in amorphous solids. *Physical Review E*, 57(6):7192, 1998.

M. J. Fuerstman, P. Garstecki, and G. M. Whitesides. Coding/decoding and reversibility of droplet trains in microfluidic networks. *Science*, 315(5813):828–832, 2007.

J. Geng, D. Howell, E. Longhi, R. P. Behringer, G. Reydellet, L. Vanel, E. Clément, and S. Luding. Footprints in sand: The response of a granular material to local perturbations. *Physical Review Letters*, 87:035506, 2001.

V. Gibiat, E. Plaza, and P. De Guibert. Acoustic emission before avalanches in granular media. *arXiv preprint arXiv:0906.3820*, 2009.

F. Gimbert, D. Amitrano, and J. Weiss. Crossover from quasi-static to dense flow regime in compressed frictional granular media. *EPL (Europhysics Letters)*, 104(4):46001, 2013.

C. Goldenberg and I. Goldhirsch. Friction enhances elasticity in granular solids. *Nature*, 435 (7039):188–191, 2005.

I. Goldhirsch and C. Goldenberg. On the microscopic foundations of elasticity. *The European Physical Journal E*, 9(3):245–251, 2002.

J. Goyon, A. Colin, G. Ovarlez, A. Ajdari, and L. Bocquet. Spatial cooperativity in soft glassy flows. *Nature*, 454(7200):84–87, 2008.

S. A. Hall, D. M. Wood, E. Ibraim, and G. Viggiani. Localised deformation patterning in 2d granular materials revealed by digital image correlation. *Granular Matter*, 12:1–14, 2010.

P. Hébraud and F. Lequeux. Mode-coupling theory for the pasty rheology of soft glassy materials. *Physical Review Letters*, 81(14):2934, 1998.

P. Hébraud, F. Lequeux, J. P. Munch, and D. J. Pine. Yielding and rearrangements in disordered emulsions. *Physical Review Letters*, 78(24):4657, 1997.

H. J. Herrmann, J. P. Hovi, and S. Luding. Physics of dry granular media. *NATO-ASI Series E 350, Kluwer academic publishers, Dordrecht*, 1998.

A. Ishimaru. *Wave Propagation and Scattering in Random Media*. Academic Press, 1978.

X. Jia, C. Caroli, and B. Velicky. Ultrasound propagation in externally stressed granular media. *Physical Review Letters*, 82:1863–1866, 1999.

M. Joanicot and A. Ajdari. Droplet control for microfluidics. *Science*, 309(5736):887–888, 2005.

F. Jousse, R. Farr, D. R. Link, M. J. Fuerstman, and P. Garstecki. Bifurcation of droplet flows within capillaries. *Physical Review E*, 74(3):036311, 2006.

A. Kabla and G. Debrégeas. Local stress relaxation and shear banding in a dry foam under shear. *Physical Review Letters*, 90(25):258303, 2003.

A. Kabla, J. Scheibert, and G. Debregeas. Quasi-static rheology of foams. part 2. continuous shear flow. *Journal of Fluid Mechanics*, 587:45–72, 2007.

K. Kamrin and G. Koval. Nonlocal constitutive relation for steady granular flow. *Physical Review Letters*, 108(17):178301, 2012.

A. S. Keys, A. R. Abate, S. C. Glotzer, and D. J. Durian. Measurement of growing dynamical length scales and prediction of the jamming transition in a granular material. *Nature physics*, 3(4):260–264, 2007.

S. Kiesgen de Richter. *Étude de l'organisation des réarrangements d'un milieu granulaire sous sollicitations mécaniques*. PhD thesis, Thèse de doctorat, Université de Rennes 1, 2009.

S. Kiesgen de Richter, G. Le Caër, and R. Delannay. Dynamics of rearrangements during inclination of granular packings: the avalanche precursor regime. *Journal of Statistical Mechanics: Theory and Experiment*, 2012(04):P04013, 2012.

D. Klaumünzer, A. Lazarev, R. Maaß, F. H. Dalla Torre, A. Vinogradov, and J. F. Löffler. Probing shear-band initiation in metallic glasses. *Physical Review Letters*, 107:185502, 2011.

T. S. Komatsu, S. Inagaki, N. Nakagawa, and S. Nasuno. Creep motion in a granular pile exhibiting steady surface flow. *Physical Review Letters*, 86(9):1757, 2001.

M. R. Kuhn. Structured deformation in granular materials. *Mechanics of materials*, 31(6):407–429, 1999.

A. Le Bouil, A. Amon, S. McNamara, and J. Crassous. Emergence of cooperativity in plasticity of soft glassy materials. *arXiv preprint arXiv:1402.7304*, 2014a.

A. Le Bouil, A. Amon, J.-C. Sangleboeuf, H. Orain, P. Bésuelle, G. Viggiani, P. Chasle, and J. Crassous. A biaxial apparatus for the study of heterogeneous and intermittent strains in granular materials. *Granular Matter*, 16(1):1–8, 2014b.

F. Lechenault, O. Dauchot, G. Biroli, and J.-P. Bouchaud. Critical scaling and heterogeneous superdiffusion across the jamming/rigidity transition of a granular glass. *EPL (Europhysics Letters)*, 83(4):46003, 2008.

R. Lehoucq, J. Weiss, B. Dubrulle, A. Amon, A. Le Bouil, J. Crassous, D. Amitrano, and F. Graner. Analysis of image versus position, scale and direction reveals pattern texture anisotropy. submitted to Journal of Statistical Mechanics: Theory and Experiment.

A. Lemaître. Rearrangements and dilatancy for sheared dense materials. *Physical Review Letters*, 89:195503, 2002.

W. Leutz and J. Rička. On light propagation through glass bead packings. *Optics communications*, 126(4):260–268, 1996.

A. J. Liu and S. R. Nagel. Jamming is not just cool any more. *Nature*, 396(6706):21–22, 1998.

C. H. Liu, S. R. Nagel, D. A. Schecter, S. N. Coppersmith, S. Majumdar, O. Narayan, and T. A. Witten. Force fluctuations in bead packs. *Science*, pages 513–513, 1995.

F. C. MacKintosh, J. X. Zhu, D. J. Pine, and D. A. Weitz. Polarization memory of multiply scattered light. *Physical Review B*, 40(13):9342–9345, 1989.

T. S. Majmudar and R. P. Behringer. Contact force measurements and stress-induced anisotropy in granular materials. *Nature*, 435(7045):1079–1082, 2005.

H. A. Makse, N. Gland, D. L. Johnson, and L. Schwartz. Granular packings: Nonlinear elasticity, sound propagation, and collective relaxation dynamics. *Physical Review E*, 70:061302, 2004.

C. E. Maloney and A. Lemaître. Amorphous systems in athermal, quasistatic shear. *Physical Review E*, 74(1):016118, 2006.

M. L. Manning and A. J. Liu. Vibrational modes identify soft spots in a sheared disordered packing. *Physical Review Letters*, 107(10):108302, 2011.

G. Maret. Diffusing-wave spectroscopy. *Current opinion in colloid & interface science*, 2(3): 251–257, 1997.

G. Maret and P. E. Wolf. Multiple light scattering from disordered media. the effect of brownian motion of scatterers. *Zeitschrift für Physik B Condensed Matter*, 65(4):409–413, 1987.

N. Menon and D. J. Durian. Diffusing-wave spectroscopy of dynamics in a three-dimensional granular flow. *Science*, 275(5308):1920–1922, 1997.

R. M. Nedderman. *Statics and kinematics of granular materials*. Cambridge University Press, 2005.

N. Nerone, M. A. Aguirre, A. Calvo, D. Bideau, and I. Ippolito. Instabilities in slowly driven granular packing. *Physical Review E*, 67:011302, 2003.

V. B. Nguyen, T. Darnige, A. Bruand, and E. Clement. Creep and fluidity of a real granular packing near jamming. *Physical Review Letters*, 107:138303, 2011.

K. Nichol, A. Zanin, R. Bastien, E. Wandersman, and M. van Hecke. Flow-induced agitations create a granular fluid. *Physical Review Letters*, 104(7):078302, 2010.

P. Oswald. *Rhéophysique. Ou comment coule la matière*. Belin, 2005.

G. Ovarlez and E. Clément. Elastic medium confined in a column versus the janssen experiment. *The European Physical Journal E*, 16(4):421–438, 2005.

G. Picard, A. Ajdari, F. Lequeux, and L. Bocquet. Slow flows of yield stress fluids: Complex spatiotemporal behavior within a simple elastoplastic model. *Physical Review E*, 71(1):010501, 2005.

D. J. Pine. *Soft and Fragile Matter: Nonequilibrium Dynamics, Metastability and Flow*, volume 53, chapter Light scattering and rheology of complex fluids driven far from equilibrium, pages 9–74. SUSSP Institute of Physics, Bristol, 2000.

D. J. Pine, D. A. Weitz, P. M. Chaikin, and E. Herbolzheimer. Diffusing wave spectroscopy. *Physical Review Letters*, 60(12):1134, 1988.

D. J. Pine, D. A. Weitz, J. X. Zhu, and E. Herbolzheimer. Diffusing-wave spectroscopy: dynamic light scattering in the multiple scattering limit. *Journal de Physique*, 51(18):2101–2127, 1990.

F. Radjai and S. Roux. Turbulentlike fluctuations in quasistatic flow of granular media. *Physical Review Letters*, 89(6):064302, 2002.

F. Radjai, M. Jean, J.-J. Moreau, and S. Roux. Force distributions in dense two-dimensional granular systems. *Physical Review Letters*, 77:274–277, 1996.

A. L. Rechenmacher. Grain-scale processes governing shear band initiation and evolution in sands. *Journal of the Mechanics and Physics of Solids*, 54(1):22–45, 2006.

K. A. Reddy, Y. Forterre, and O. Pouliquen. Evidence of mechanically activated processes in slow granular flows. *Physical Review Letters*, 106(10):108301, 2011.

G. Reydellet. *Mesure expérimentale de la fonction réponse d'un matériau granulaire*. PhD thesis, Thèse de doctorat, Université Paris 6, 2002.

G. Reydellet and E. Clément. Green's function probe of a static granular piling. *Physical Review Letters*, 86:3308–3311, 2001.

K. H. Roscoe. The influence of strains in soil mechanics. *Géotechnique*, 20:29–170, 1970.

S. M. Rubinstein, G. Cohen, and J. Fineberg. Dynamics of precursors to frictional sliding. *Physical Review Letters*, 98:226103, 2007.

P. Schall and M. van Hecke. Shear bands in matter with granularity. *Annual Review of Fluid Mechanics*, 42(1):67, 2009.

P. Schall, D. A. Weitz, and F. Spaepen. Structural rearrangements that govern flow in colloidal glasses. *Science*, 318(5858):1895–1899, 2007.

F. Scheffold and R. Cerbino. New trends in light scattering. *Current Opinion in Colloid & Interface Science*, 12(1):50–57, 2007.

M. Schindler and A. Ajdari. Droplet traffic in microfluidic networks: A simple model for understanding and designing. *Physical Review Letters*, 100(4):044501, 2008.

C. P. Schofield, A. N.; Wroth. *Critical State Soil Mechanics*. McGraw-Hill, 1968.

C. A. Schuh, T. C. Hufnagel, and U. Ramamurty. Mechanical behavior of amorphous alloys. *Acta Materialia*, 55(12):4067–4109, 2007.

D. A. Sessoms, M. Belloul, W. Engl, M. Roche, L. Courbin, and P. Panizza. Droplet motion in microfluidic networks: Hydrodynamic interactions and pressure-drop measurements. *Physical Review E*, 80(1):016317, 2009.

D. A. Sessoms, A. Amon, L. Courbin, and P. Panizza. Complex dynamics of droplet traffic in a bifurcating microfluidic channel: Periodicity, multistability, and selection rules. *Physical Review Letters*, 105(15):154501, 2010a.

D. A. Sessoms, H. Bissig, A. Duri, L. Cipelletti, and V. Trappe. Unexpected spatial distribution of bubble rearrangements in coarsening foams. *Soft Matter*, 6(13):3030–3037, 2010b.

S. E. Skipetrov, J. Peuser, R. Cerbino, P. Zakharov, B. Weber, and F. Scheffold. Noise in laser speckle correlation and imaging techniques. *Optics Express*, 18(14):14519–14534, 2010.

P. Sollich. Rheological constitutive equation for a model of soft glassy materials. *Physical Review E*, 58(1):738, 1998.

P. Sollich, F. Lequeux, P. Hébraud, and M. E. Cates. Rheology of soft glassy materials. *Physical Review Letters*, 78(10):2020, 1997.

E. Somfai, J.-N. Roux, J. H. Snoeijer, M. van Hecke, and W. van Saarloos. Elastic wave propagation in confined granular systems. *Physical Review E*, 72:021301, 2005.

F. Spaepen. A microscopic mechanism for steady state inhomogeneous flow in metallic glasses. *Acta metallurgica*, 25(4):407–415, 1977.

L. Staron, J.-P. Vilotte, and F. Radjai. Preavalanche instabilities in a granular pile. *Physical Review Letters*, 89(20):204302, 2002.

L. Staron, F. Radjai, and J.-P. Vilotte. Granular micro-structure and avalanche precursors. *Journal of Statistical Mechanics: Theory and Experiment*, 2006(07):P07014, 2006.

H. A. Stone, A. D. Stroock, and A. Ajdari. Engineering flows in small devices: microfluidics toward a lab-on-a-chip. *Annual Review of Fluid Mechanics*, 36:381–411, 2004.

P. Tan, N. Xu, A. B. Schofield, and L. Xu. Understanding the low-frequency quasilocalized modes in disordered colloidal systems. *Physical Review Letters*, 108(9):095501, 2012.

A. Tanguy, J. P. Wittmer, F. Leonforte, and J.-L. Barrat. Continuum limit of amorphous elastic bodies: A finite-size study of low-frequency harmonic vibrations. *Physical Review B*, 66(17): 174205, 2002.

A. Tanguy, F. Leonforte, and J.-L. Barrat. Plastic response of a 2d lennard-jones amorphous solid: Detailed analysis of the local rearrangements at very slow strain rate. *The European Physical Journal E*, 20(3):355–364, 2006.

A. Tordesillas. Force chain buckling, unjamming transitions and shear banding in dense granular assemblies. *Philosophical Magazine*, 87(32):4987–5016, 2007.

M. Tsamados, A. Tanguy, F. Léonforte, and J.-L. Barrat. On the study of local-stress rearrangements during quasi-static plastic shear of a model glass: Do local-stress components contain enough information? *The European Physical Journal E*, 26(3):283–293, 2008.

M. Tsamados, A. Tanguy, C. Goldenberg, and J.-L. Barrat. Local elasticity map and plasticity in a model lennard-jones glass. *Physical Review E*, 80(2):026112, 2009.

H. C. van de Hulst. *Light scattering by small particles*. Courier Dover Publications, 1981.

M. Van Hecke. Jamming of soft particles: geometry, mechanics, scaling and isostaticity. *Journal of Physics: Condensed Matter*, 22(3):033101, 2010.

L. Vanel, D. Howell, D. Clark, R. P. Behringer, and E. Clément. Memories in sand: Experimental tests of construction history on stress distributions under sandpiles. *Physical Review E*, 60(5): R5040, 1999.

V. Viasnoff, F. Lequeux, and D. J. Pine. Multispeckle diffusing-wave spectroscopy: A tool to study slow relaxation and time-dependent dynamics. *Review of Scientific Instruments*, 73, 2002.

G. Viggiani and S. A. Hall. Full-field measurements in experimental geomechanics: historical perspective, current trends and recent results. *Advanced experimental techniques in geomechanics*, pages 3–67, 2004.

D. A. Weitz and D. J. Pine. *Diffusing-wave spectroscopy*, chapter Dynamic Light Scattering : The Method and Some Applications. Oxford University Press, 1993.

P. Welker and S. McNamara. Precursors of failure and weakening in a biaxial test. *Granular Matter*, 13(1):93–105, 2011.

X. L. Wu, D. J. Pine, P. M. Chaikin, J. S. Huang, and D. A. Weitz. Diffusing-wave spectroscopy in a shear flow. *J. Opt. Soc. Am. B*, 7(1):15–20, 1990.

M. Wyart, S. R. Nagel, and T. A. Witten. Geometric origin of excess low-frequency vibrational modes in weakly connected amorphous solids. *EPL (Europhysics Letters)*, 72(3):486, 2005.

N. Xu, M. Wyart, A. J. Liu, and S. R. Nagel. Excess vibrational modes and the boson peak in model glasses. *Physical Review Letters*, 98(17):175502, 2007.

V. Y. Zaitsev, P. Richard, R. Delannay, V. Tournat, and V. E. Gusev. Pre-avalanche structural rearrangements in the bulk of granular medium: Experimental evidence. *EPL (Europhysics Letters)*, 83(6):64003, 2008.

P. Zakharov and F. Scheffold. Monitoring spatially heterogeneous dynamics in a drying colloidal thin film. *Soft Materials*, 8(2):102–113, 2010.